KARST SYSTEM IDENTIFICATION BY PROCESS - BASED MODELLING. THE CASE OF AUTA SPRING, MALAGA-SPAIN

By

Sammy Gregory Ramirez Yauri

A Thesis submitted in partial fulfilment of the requirement for the degree of:

MSc. Water Resources and Environment

Supervisors

Dr. Bartolome Andreo (Center of Hydrogeology at University of Malaga - Spain, CEHIUMA)

Dr. Andreas Hartmann (Institute of Hydrology at University of Freiburg - Germany)

ACKNOWLEGDEMENTS

I would like to thank my supervisor Dr. Bartolome Andreo Navarro from The University of Malaga for giving me this opportunity, for his suggestions, and his support to finish my work.

I would like to express my sincere gratitude and appreciation, Dr. Andreas Hartmann from The University of Freiburg - Institute of Hydrology for all the guidance he has provided to me along each step of the project, his professional support, his practical way and his infinite understanding and mental support. He now became a very good friend.

I thank to Dr. Matías Mudarra because he provided the data used for modeling developed in the frame of this Master thesis.

I am grateful to Prof. Markus Weiler for accepting me and giving me a nice place to work along of this period.

Thanks for the friendship of my friends at the Institute of Hydrology and special thanks to Fabian Ries, Daphné Freudiger and Nina Baldinger who make me feel at home.

Many thanks to my parents Marilú and Andres for their patience and for giving me encouragement during my study.

ABSTRACT

The karst springs are an important source of drinking water for the population of the Malaga province. It is important to know the capacity, the chemical quality, boundary conditions, and flow dynamics of karst aquifer as well as able to understand the functioning to can take actions for exploitation or prevention. For this study the data were obtained from a previous study at the Center for Hydrogeology of Malaga (Mudarra 2012).

Los Tajos-Sierra de Enmedio aquifer is located in South of Spain, north-east of the city of Malaga with a recharge area of 8.98 km^2. Sabar River is located in the north-east of the aquifer and the De la Cueva River is located in the south -west edge. The geology of the study area is made up by limestone, marly-limestones and dolomites which display some karst forms on the surface. The hydrochemistry confirms the contact of water with the calcareous rock spring. There was also a test tracer test that confirmed the connection between Sabar River and Los Tajos-Sierra de Enmedio aquifer (Mudarra 2012).

To represent the physical environment in the most realistic way, four storages are built. The first storage is comprised by the soil and epikarst which together are *Overflow storage*. The second storage is comprised by the unsaturated zone which is *Linear Reservoir storage*. The third storage is comprised by the matrix and conducts (saturated zone) which together are *Linear Exchange storage*. The fourth storage is comprised by the Sabar River which is *river storage*.

Four models are built with different possibilities connections to the river storage (Sabar River). The first model is called *Exchange model* and considered three storages and without influence of the river storage. This model represents the basic model and identifying the differences with other models. The second model is called *Exchange-river-vadose zone model* and considered the four storages but the river storage is connected with the unsaturated zone. The third model is called *Exchange-river-matrix model* and considered the four storages but the river storage is connected with the matrix of the linear exchange storage. The fourth model is called *Exchange-river-conduits model* and considered the four storages but the river storage is connected with the conduits of the linear exchange storage.

The models were calibrated by Shuffled Complex Evolution of the University of Arizona (SCE-UA) which is a method of self-calibration and shows the best value for each parameter. Efficiency Nash Sutcliffe (NSE) is used to measure the performance of the model between 0-1 (near 1 is the best), Sensitivity analysis is a method to identify which parameters are more sensitive and influence in the result. Percentage of recharge method

is used to identify whether the recharge water is in the range of reality. Finally Monte Carlo sampling made several iterations (10000 in this case) to find the best fit.

The results of the last three models were similar to the basic model, the efficiency coefficient of the all the models are good, and the sensitivity analysis shows that only the three same parameters of all models are sensitive, and Monte Carlo Sampling also gave similar results to sensitivity analysis. It can be concluded that the range of uncertainty in the recharge area is high and that only measures discharge of Auta spring are not enough. It is necessary improve the numerical conceptual model for the best characterization to the river influence. Should make a chemical modeling to be sure how much percentage of the river participates in aquifer recharge.

RESUMEN

Los manantiales kársticos son una fuente importante de consumo de agua para la población de la provincia de Málaga. Es importante saber la capacidad, la calidad hidroquímica, condiciones de contorno, la dinámica del flujo para entender el funcionamiento de los acuíferos kársticos y aplicar acciones de explotación o prevención. Para la zona de estudio los datos obtenidos eran de un estudio previo del Centro de Hidrogeología de la Universidad de Málaga (Mudarra, 2012).

El acuífero de Los Tajos-Sierra de Enmedio se localiza en el sur de España, al noreste de la ciudad de Málaga, con un área de recarga de 8.98 km^2. En la parte noreste del acuífero se encuentra el Rio Sabar y al suroeste el acuífero el Rio de la Cueva. La geología de la zona está formada por calizas, margo-calizas y dolomitas sobre las que se desarrollan algunas formas kársticas en la superficie. La hidroquímica confirma el contacto del agua con las rocas carbonatadas. También se hizo una prueba de trazadores que confirmo la conexión del rio Sabar con el acuífero de Los Tajos-Sierra de En medio (Mudarra, 2012).

Con el fin de representar el medio físico en la forma más realista, se han planteado cuatro almacenamientos. El primero almacenamiento es comprendido por el suelo y el epikarst que juntos constituyen lo que se denomina *Overflow storage*. El segundo almacenamiento es comprendido por la zona no saturada lo que se denomina *Linear reservoir storage*. El tercer almacenamiento es comprendido por la matriz y conductos (zona saturada) que juntos constituyen lo que se denomina *Linear Exchange storage*. El cuarto almacenamiento es comprendido por el rio Sabar lo que se denomina *River storage*.

Cuatro modelos fueron construidos con diferentes posibilidades de conexión con el *River storage* (rio Sabar). El primer modelo es llamado *Exchange model* y considera tres almacenamientos pero sin la influencia del River storage (rio Sabar). Este modelo representa el modelo base identificando la diferencia con los otros modelos. El segundo modelo es llamado *Exchange-river-vadose zone model* y considera los cuatro almacenamientos pero el *River storage* está conectado con la zona no saturada. El tercer modelo es llamado *Exchange-river-matrix model* y considera los cuatro almacenamientos pero el River storage está conectado con la matriz de *Linear exchange storage*. El cuarto modelo es llamado *Exchange-river-conduits model* y considera los cuatro almacenamientos pero el River storage está conectado con los conductos de *Linear exchange storage*.

Para calibrar los modelos se utilizó el método de Evolución y Mezcla Compleja de la Universidad de Arizona (SCE-UA), es un método de auto calibración y muestra el mejor valor para cada parámetro. Para la validación del modelo se utilizó Eficiencia de Nash

Sutcl-iffe (NSE) es un coeficiente que mide el rendimiento del modelo entre 0 – 1 (cerca de 1 es mejor), Análisis de sensibilidad es un método para identificar que parámetros son más sensibles e influyen en el resultado. Porcentaje de recarga este método sirve para identificar si la recarga de agua está en el margen de la realidad y por ultimo muestreo de Monte Carlo que realiza muchas iteraciones (10000 en este caso) para encontrar el mejor ajuste.

El resultado de los tres últimos modelos fueron similares con el modelo base, los coeficientes de rendimiento en todo los modelos son muy buenos, el análisis de sensibilidad mostro solo tres parámetros iguales en todo los modelos eran sensibles, Muestreo Monte Carlo también dio resultados parecidos al de análisis de sensibilidad. Donde se concluyó que el rango de incertidumbre en el área de recarga es elevada, como también solo las medidas de descarga del manantial de Auta no son suficientes, es necesario mejorar el modelo conceptual numérico para la mejor caracterización de la influencia del rio. Se debería hacer un modelado químico para estar seguro cuánto del porcentaje del rio participa en la recarga del acuífero.

LIST OF CONTENTS

LIST OF FIGURES

LIST OF TABLES

1 INTRODUCTION

1.1. GENERAL INTRODUCTION

Water is the most abundant substance on the earth, the principal constituent of the life in the earth. Therefore it is a key factor for the human existence and the civilization process. The hydro-sciences deal with the earth's water resources with respect the distribution, circulation, physical, chemical properties, and interaction with the environment furthermore including the interaction with other living things and humans. Many cities around of Spain and Andalucía zone are using the ground water for agriculture, livestock and human use.

In the last decades the groundwater model investigation has been increased rapidly with the growing environmental software. The ground water models investigation have developed from quantifying the groundwater resources of groundwater exploration, problems with three-dimensional flow and transport, and identifying the true influence of the boundary conditions. Many numerical models have been developed to solve a long variety of problems. That is the reason the best choose are considered to have the important requirement for each model. The requirements are how many information have to develop the model. Commonly are inputs, outputs and geography information.

In the present groundwater problem is identifying the influence of the river in the spring discharge. One method to evaluate this problem is to apply numerical models. Lumped model is applied with the software ''MatLab''. This method is efficient, fastest, and simplest. The best model is most simple as possible also consider how many parameters have the model. In this case just the inputs (precipitation, and Sabar river recharge), and the outputs (real evapotranspiration, and discharge of the Auta spring).

Based in lumped numerical model, calibrated with The Shuffled Complex Evolution (SCE-UA), evaluated with Nash Sutcliffe efficiency (NSE), Sensitivity analyst, recharge rate and Monte Carlo sampling have been used. This report evaluated four possible conceptual numerical models, and shows many of the difficulties to understand and to interpret the results.

2 KARST HYDROGEOLOGY

2.1. DEFINITION

Karst describes special forms of landscapes containing caves, sinkholes, poljés characterized by great groundwater systems that are developed in dissolution bedrocks for example limestones, dolostones, gypsum and halite. These landforms are indicators to identify hydrological behavior of outcrop rocks. These rocks have two types of porosity. The primary porosity is consolidated with inter granulate porosity including all class of small voids between the crystals, grains, and fossil fragments (inter crystalline, inter granulate or interstitial porosity) it consist the matrix porosity without external alteration. The secondary porosity is defined by fracturing and the dissolution of the bedrock. This generates preferred conduits and is due to the reaction of the outcrop rock with the water generating the process of karstification.

The dissolution of rocks is the interaction between water and rock over a long period of time, and it depends on the concentration of CO_2 in the water. The following chemical equation (Eq. 1.1) describes the dissolution of limestone:

$$\mathrm{CaCO_3 + H_2O + CO_2 \leftrightarrow Ca^{+2} + 2HCO3^{-2}} \text{ Eq. 1.1}$$

The presence of CO2 in water increases the solubility of limestones. The rainfall interacts with atmosphere when it fall down and in the same time it dissolves the CO_2 and the rates increasing. Furthermore soil processes such as respiration of plant roots and decomposition of buried plants also increase the CO_2 concentration. In the equation the presence of CO_2 in the water generates as a result the solubility of calcium Ca and bicarbonate HCO_3 (Ford, D. C., & Williams, P. W. (2007).

When the process of karstification is well developed a good connection between wider network conduits and outputs allows rapid and often turbulent water flows and therefore the calcite dissolution as well as the percentage of calcium in water is increased.

2.2. KARST HYDROLOGY

A karst system is divided in four sub systems. The first sub system is characterized by two sorts of recharge, an autogenic recharge area and an allogenic recharge area. The autogenic system includes internal runoff and diffuse infiltration, which are both directly in contact with the recharge area. The allogenic recharge area consists of external runoff and streams that contribute to the autogenic recharge area. The flow enters then the second sub system that is constituted by soil and epikarst. In this sub system the water is stored and the flow is concentrated due to the soil that was developed into carbonate rock and it had content of clay. Afterwards, the flow enters the third sub system which is an unsaturated zone or a vadose zone. The water flows through conduits or matrix. The water flow into the conduits generates faster and often turbulent flow, in contrary the matrix is slower. It can occur that the water flow from the matrix to the conduits and vice versa. Finally, the fourth sub system is a saturated zone where the discharge is represented by one or more main springs. Depending on level of karstification, the system can have one or more overflow springs that are activated when the capacity of the conduits are exceeded. Commonly overflow springs are located above the main spring discharge. However karstification is a complex process and different situations can occur (Figure 1).

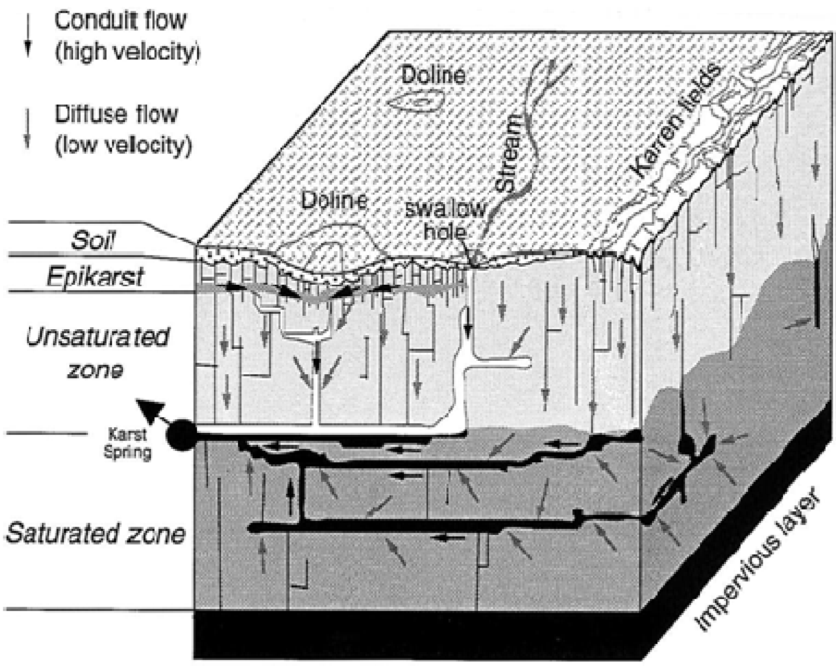

Fig 1 Conceptual model of a karst aquifer (Doerfliger and Zwahlen 1995)

2.3. TYOE OF MODELS

Hydrological models can be classified in various types. One of the classification method used by is Chow (1988). In this classification the models are primarily separated in two major hydrological models groups, stochastic and deterministic (Figure 2).

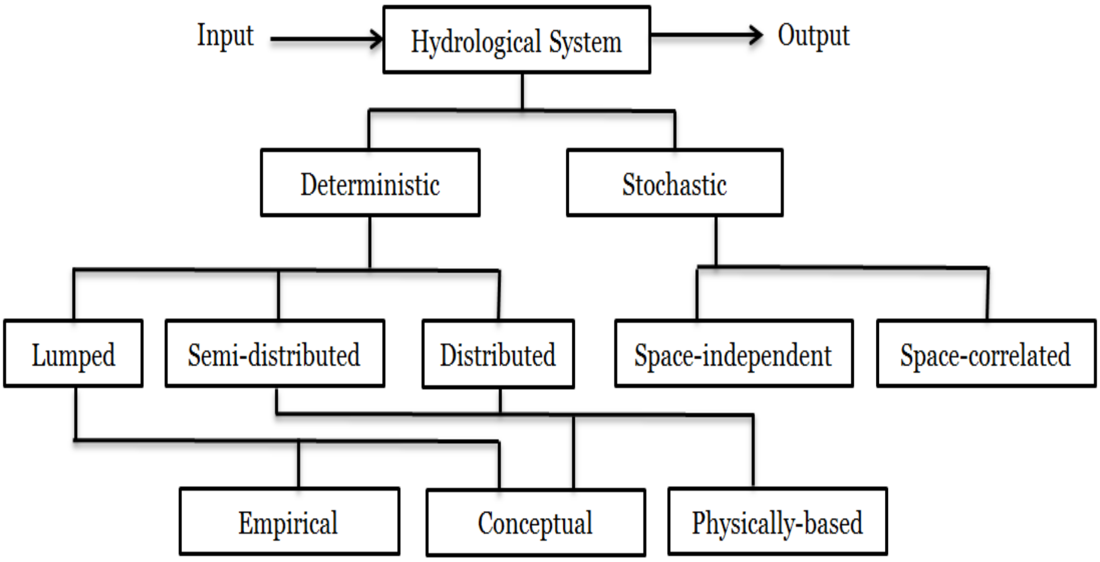

Fig 2 Classification of Hydrological models (Chow et al 1988).

Stochastic models are regarded as black-box systems, the black-box systems indicate that the inputs and the outputs are assimilated but without any knowledge about the internal process. Furthermore the inputs are linked to the outputs using mathematical and statistical concepts. These processes are determined by probabilistic theories, which every model with statistical probabilistic are stochastic model.

The deterministic models are sometimes referred to as white-box system or grey-box system. The white-box systems or physically based models represent exactly the reality in mathematical equations. One advantage of these models is that they have a good performance if the study area has a large amount of data available and if the area is small. On the opposite, the disadvantage of such models is that they require complicated numerical solving techniques and large amount of input data. The grey-box systems do not represent all the hydrological processes as the white systems because they are based on simplified equations and partially know.

Within deterministic models, Lumped models consider more simplified space inside the study area. Each parameter in the model is uniform over the entire area (catchment area) and the water flows are represented with boxes of water reservoirs. These boxes area usually soil storage, vadose zone, matrix etc. The natural flow among the boxes is set by parameters and equations. The lumped models are calibrated comparing among the simulated data with the observed data. The observed data could be the discharge of the rivers, the springs or both in the same time. The river can contribute to the discharge or to the recharge of the aquifer, but in this case of study, the discharge of Sabar River partially recharges the aquifer.

The semi--distributed models divide the study area in sub-catchments that are treated homogeneously within them. Parameters are set for each sub-catchment and the water flows between them. The discharge is measured for the river system and is then compared to the modeled data (Figure 3).

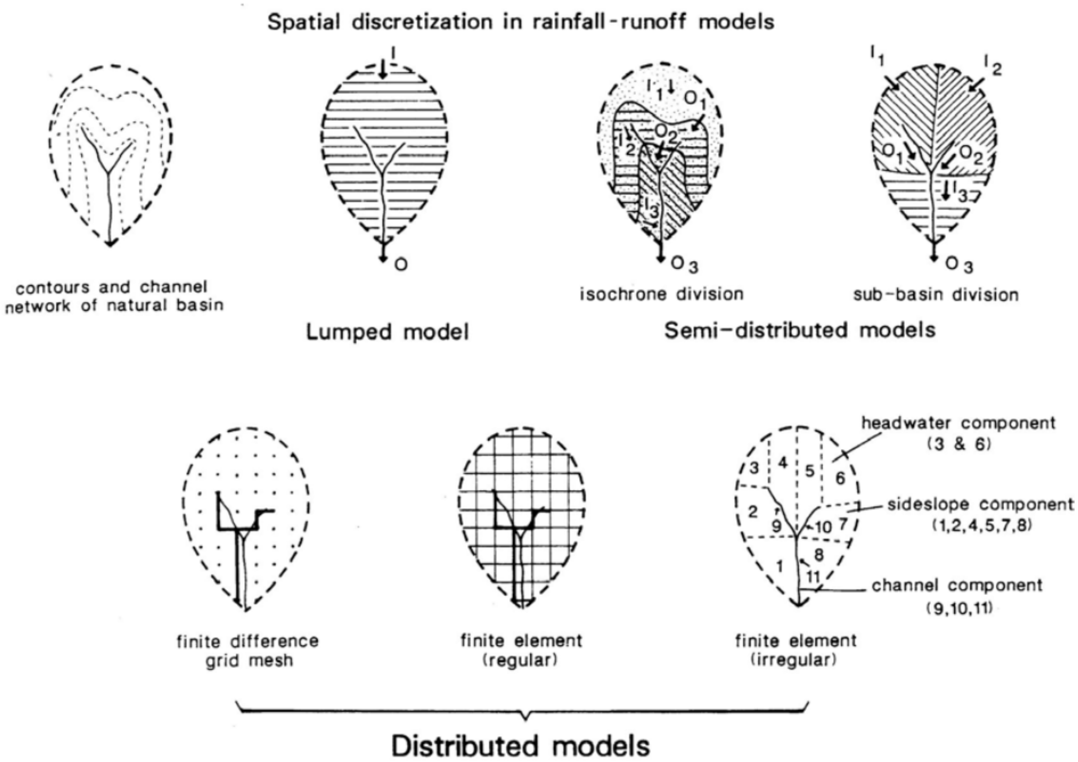

Fig 3 Graphic representation of geometrically – distributed and lumped models. (From Jones, 1997). I is the input and O is the output.

The distributed models consider that the study area (catchment) is divided into elementary units like a grid and that the water flows from one grid point (node) to another representing the water through the surface in the study area (catchment).

3 OBJECTIVES OF THIS WORK

3.1. MAIN OBJECTIVE

- Quantify the Sabar River contribution to the aquifer Los Tajos-Sierra de Enmedio by numerical model in the software Matlab and comparison between each of them furthermore using discharge data for the calibration and validation with different methods.

3.2. SECONDARY OBJECTIVES

- Define the numerical conceptual model considered each part of the aquifer as a storage and make different connect assumptions between the Sabar River and the other storages.
- Develop different karst models to represent the realistic behavior between the Sabar River and the aquifer.
- Calibration and validation of karst models that include the evaluation of the parameter sensitivity, the fit coefficient, and the real recharge rate.

4 STUDY AREA

4.1. GEOGRAPHICAL SETTING

4.1.1 Location

Los Tajos-Sierra de Enmedio aquifer are located in south Spain and north-east of Malaga city between the 4°18' - 4°14' W longitude and the 36°56'- 36°59' N latitude respectively 384000-390000 E and 4090000-4094000 N for the Zone 30 referenced on the Universal Transversal Mercator (UTM). The study area is approximately 8.98 Km^2. The topography is rugged and has altitudes ranging from 600 to 1400 meters above sea level (m.a.s.l.). The location of the Los Tajos aquifers is shown in Figure 4

The study area has two important rivers, the de la Cueva River and the Sabar River. The Sabar River is located in the north-eastern part of the study area and the de la Cueva River is located in the south-western part.

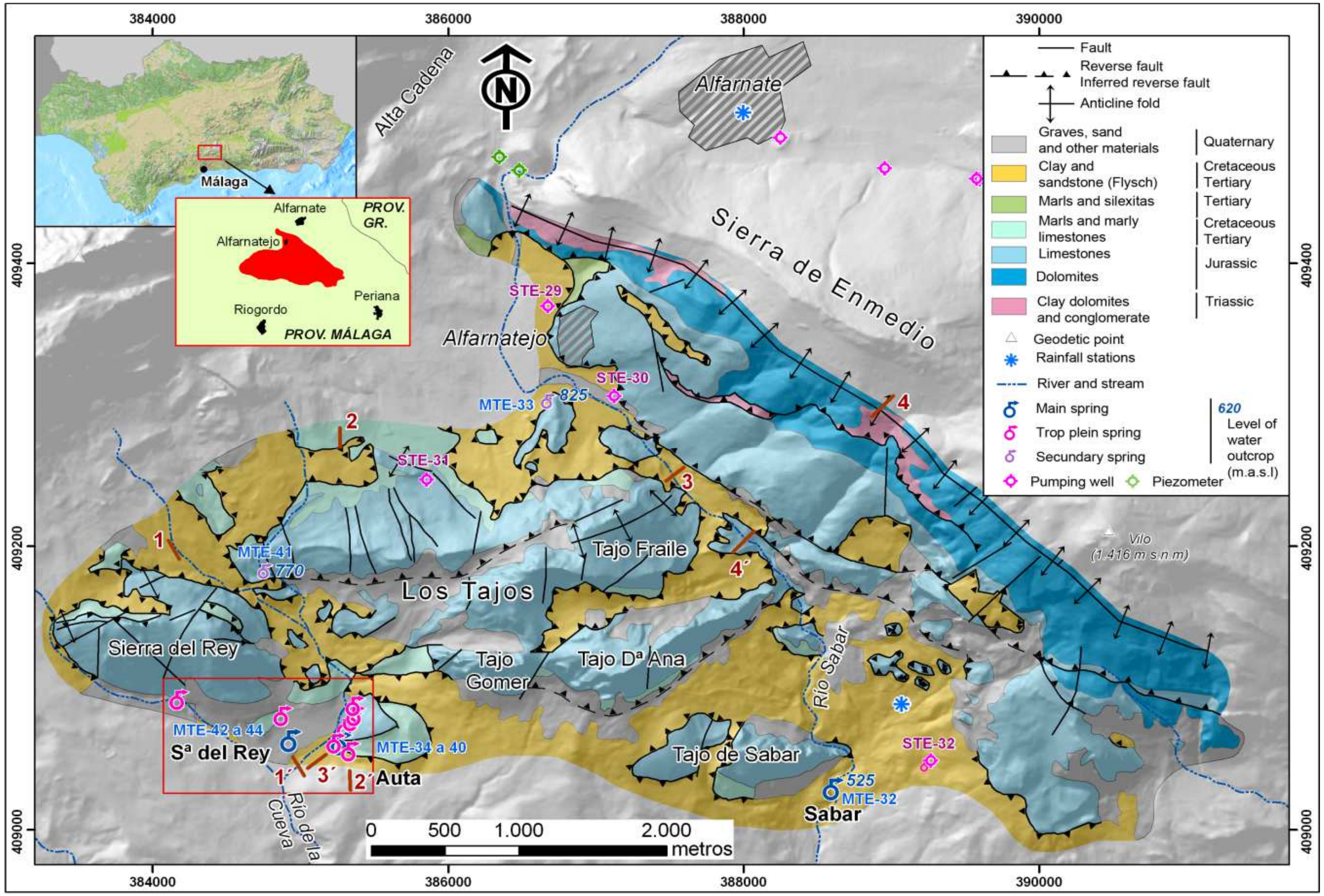

Fig 4 Geographic location and geological-Hydrogeological sketch of the study area Sierra de Enmedio-Los Tajos. The red rectangle marks the Auta spring and trop pleins. (Mudarra and Andreo 2012)

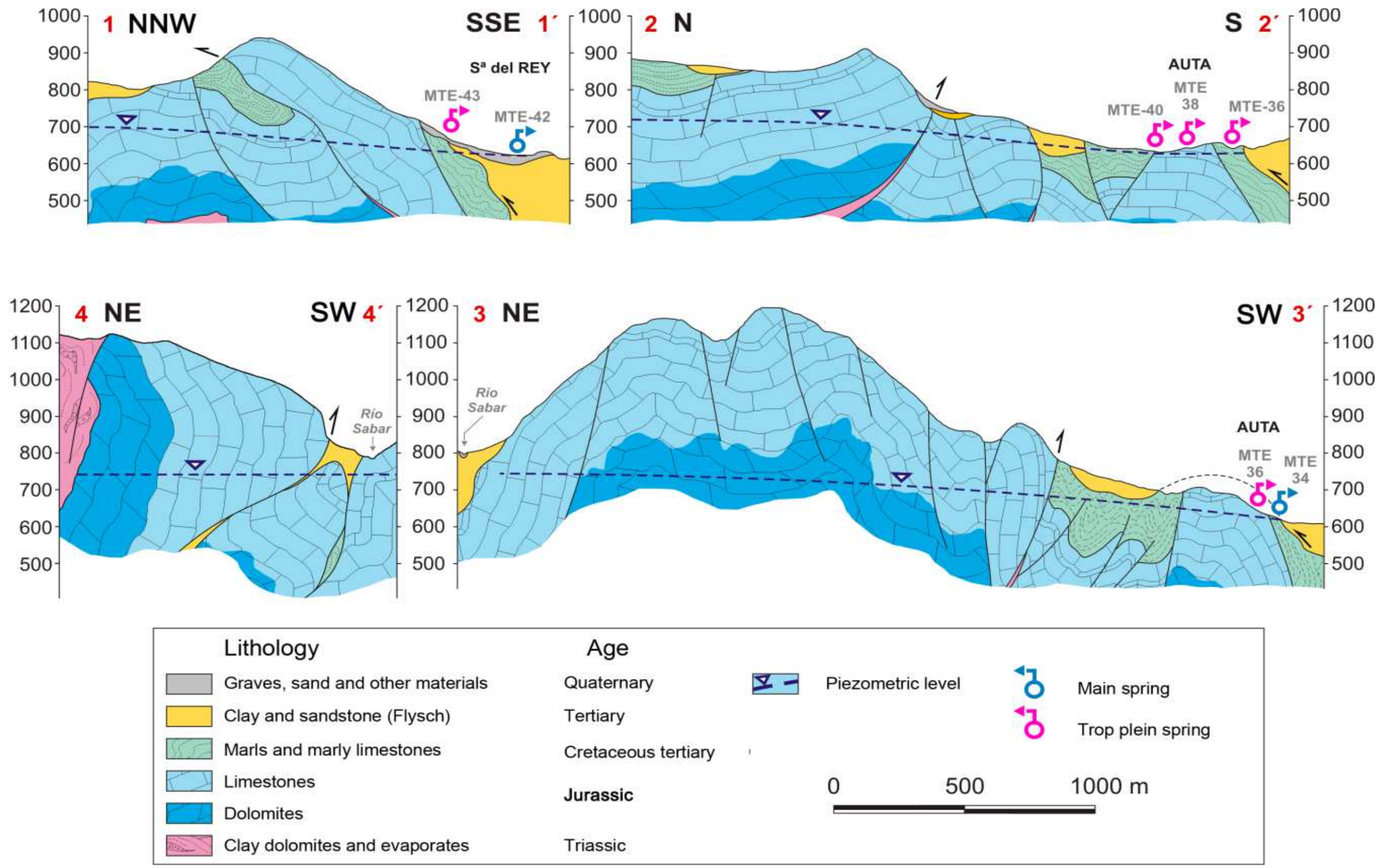

Fig 5 Cross section of geological-hydrogeological sketch of the Sierra de Enmedio-Los Tajos study area (Mudarra and Andreo 2012)

4.1.2 Climate and Temperature

The climate in the study area is mild Mediterranean. Rainfall is mainly occurring in autumn, winter and spring. It is associated with humid winds from the Atlantic. There is a pluviometric station in the study are, at the village of Alfarnate (Figure 4). The station is located in 389070 E, 4090886 N, at an elevation of 665 meters above sea level (m.a.s.l).

The historic mean annual precipitation is 650 mm (Mudarra and Andreo, 2007). However the value recorded during the study period (October 2006 - March 2009) was 751 mm (data from rain gauge station Alfarnate, Figure 4)

There is another meteorological station located in Archidona (373970 E, 4107400 N), at 529 meters above sea level (m.a.s.l). The historic average temperature in the period of time (October 2006 - March 2009) is 14 °C; this data was recovered by Junta de Andalucía - Counseling of Agriculture, Fisheries and Rural Development (Table 3.1).

	Jan	Feb	Mar	Apr	May	Jun	Jul	Aug	Sep	Oct	Nov	Dec
Mean Max. Temperature (T°)	14.10	15.38	18.04	19.38	23.05	30.04	34.43	33.92	28.15	23.37	17.58	13.91
Mean Min. Temperature (T°)	0.54	3.62	2.80	5.77	8.52	11.67	13.96	14.59	13.29	9.85	3.93	0.83
Mean Temperature (T°)	6.49	9.24	10.31	12.76	15.89	21.47	25.01	24.77	20.42	16.29	9.98	6.55
Mean wind speed (Km/h)	0.74	0.96	1.11	1.04	0.96	0.97	0.97	0.97	0.83	0.80	0.69	0.70
Mean Relative Humidity (%)	79.72	76.28	66.80	67.05	64.98	49.69	40.14	42.77	61.00	68.06	75.22	79.23

Table 1 Monthly Climatic Average Data of Archidona station

The temperature decreases with increasing elevation in the study area. Annually, the lowest temperatures are between October and March and the rest of the year the temperature are increasing. The highest measured temperature is 39.9 °C and the lowest is -5.6 °C, the variation of the climatic variables precipitation and temperature between 2006 and 2009 is shown in Figure 6

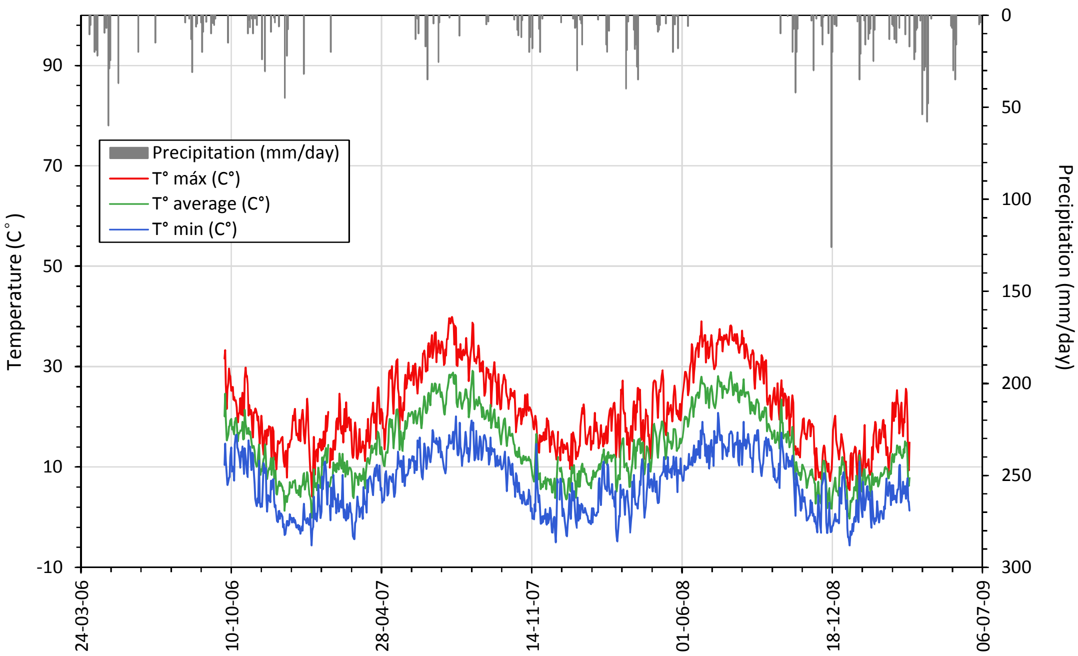

Fig 6 Temperature and rainfall of the Sierra de Enmedio – Los Tajos study area, temperature registered by hydrometereological Archidona station (Junta de Andalucía – Counseling of Agriculture, Fisheries and Rural Development).

4.2. GEOLOGICAL SETTING

The geology in the study area consists of several stratigraphic groups. It begins with Upper Triassic clays and evaporites then continues with Jurassic limestone and dolostones and finally with lower Cretaceous marls and marly-limestones.

In the north eastern part of study area Jurassic limestones and dolostones outcrop over Triassic outcrops. In the left side of the Sabar River Los Tajos area is located on the right side of the Sabar River and on the center of the study area. In this zone Jurassic outcrop is found on the higher slopes and Cretaceous tertiary outcrop on the lower slopes. The last one consist marls and marly limestones.

The geological structure of Los Tajos is formed by E-W anticline. The core of which is some overthrusts vergent toward the south, affecting clay and marly materials. To the south and north orientation the outcrop clay and sandstones (Flysch) occur (Figure 5). These materials are present within the major fractures. While in Sierra de Enmedio is oriented NW-SE. Normal and inverse faults also exist. This zone present high develop of landforms especially in the higher areas. The landforms are large karrenfields and dolines that are developed following the faults. Epikarst are formed in several parts in bare carbonate rock. The thickness of soil is found irregular in tens of centimeters. Consequently the vegetation is scarce in the Mediterranean zone.

4.3. HYDROGEOLOGY

Los Tajos and La Sierra de Enmedio comprise mainly of Jurassic limestones and dolostones that were normally fractured by tectonic movements before they were karstified. This process develops preferential conduits and landforms in the epikarst like karrenfields, dolines and uvalas. Commonly the Jurassic limestones and dolostones are identified as a recharge zone with faster infiltration due to the presence of these landsforms. Furthermore the study area has a river in the north eastern part that probably works like a border condition and consequently recharges the aquifer (Figure 7).

Outcrops of Flysch type clay and sandstone are also found close to the rivers and have a lower percentage of permeability. It shows the development of the springs between the Jurassic and Flysch lithology. This springs (Auta spring) have trop pleins springs is due to the continuous karstification and the decreasing ground water level besides. These trop pleins are active in wet period and inactive in dry period of the hydrological cycle (Figure 5).

4.3.1 Drainage

The primary mechanisms of discharge are via evapotranspiration, groundwater discharge to the river, adjacent aquifers and finally to springs.

The landforms are connected with conduits and matrix in the study area that induce an important flow within the aquifers. In the north eastern site of the study area, direct infiltration occurs through the Sabar River draining part of the flow into the aquifer and another part downstream. This was verified with a tracer test (Mudarra

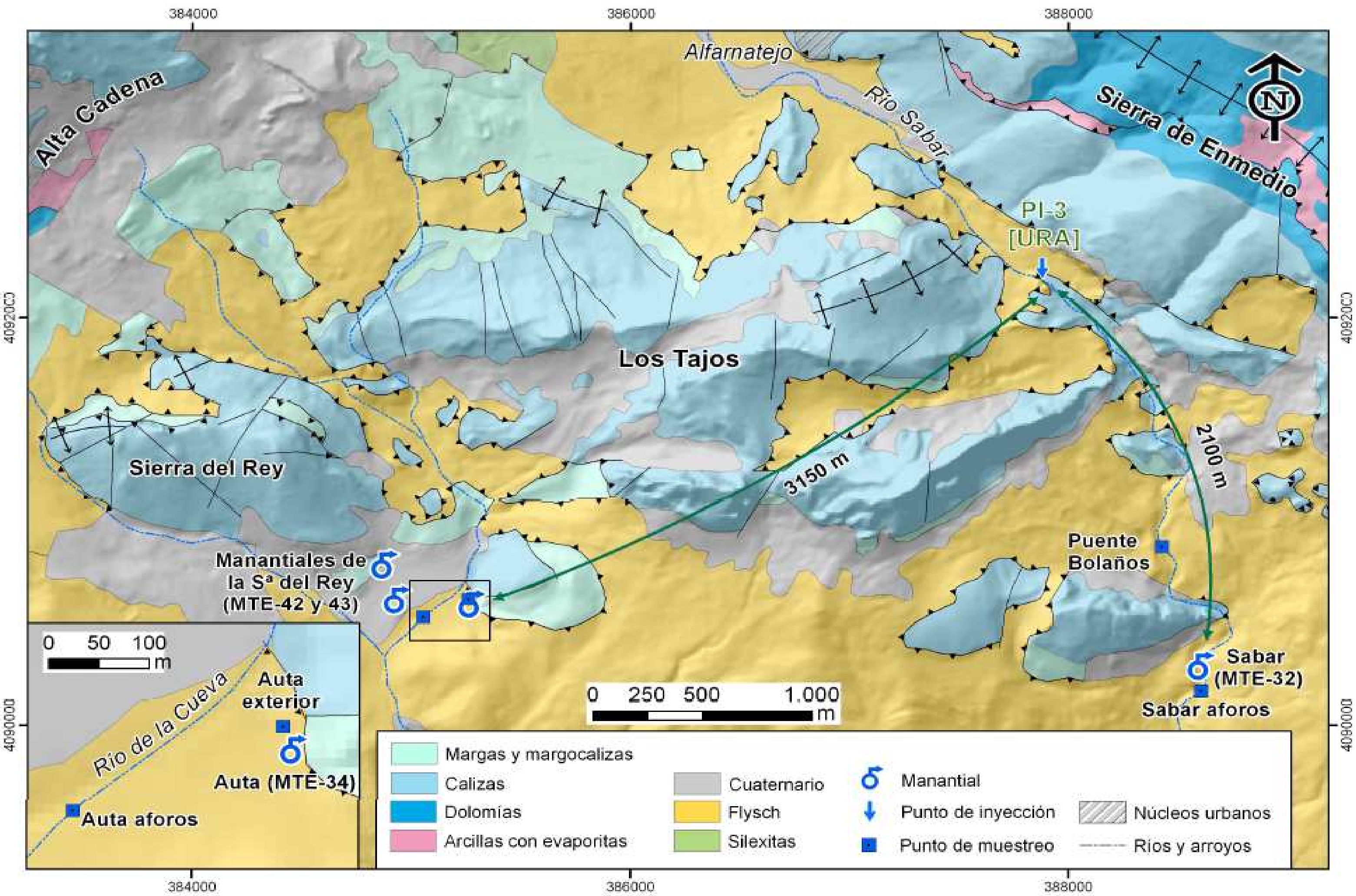

Fig 7 Test tracer in the Study Area (Mudarra, Chapter 4)

and Andreo 2012). The De la Cueva River in the south western site of the study area receives the discharge of the Auta spring to downstream.

4.3.2 Auta Spring

Auta springs are located in the south western part of the study area in 385272 E – 4090608 N UTM between the Los Tajos and Sierra del Rey aquifers (Figure 4) at an elevation 620 m.a.s.l. The Auta spring emerges between Cretaceous marl, and marly-limestones close to outcrop of limestones. This spring present five trop pleins which are active in wet periods. Furthermore in these periods the main spring is the preferred discharge path. The recorded data consider the Auta spring and the trop pleins springs together (Figure 7).

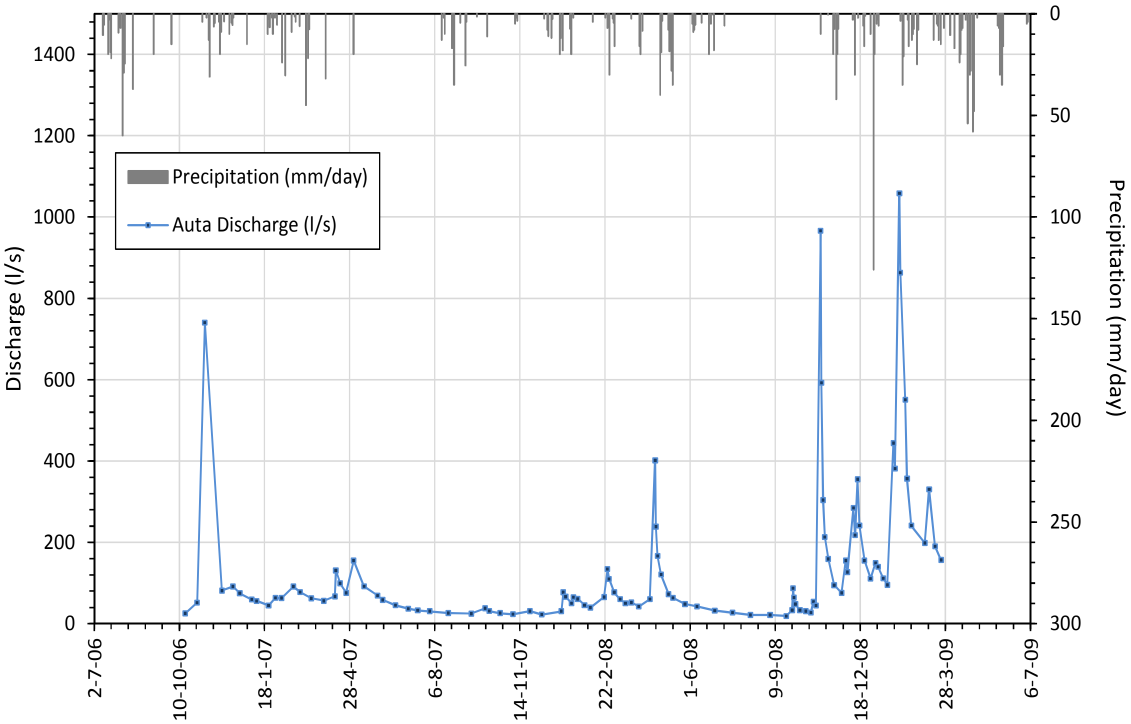

Fig 8 Hydrograph of the Auta spring and the precipitation registered by the hydrometereological Alfarnate station data obtained (Mudarra and Andreo 2012).

4.4. HYDROCHEMISTRY

The chemical data were recorded from February 2008 to March 2009 (Mudarra and Andreo 2012; Mudarra, 2012). The frequency of measure depends on the discharge intensity of the springs. Furthermore it has a good relation with the rainfall event. The time interval (frequency of measure) is namely bigger when the discharge and water level are lower (daily or once or twice a week) and in contrary the time interval is shorter when the discharge and water level are higher (hourly or daily). Furthermore the time intervals depend directly on the precision that is needed in the study area.

The measure also consider water temperature (T°), pH electrical conductivity (EC), total alkalinity (Alk) and chemical analyses of the major components ($Ca^{2+,}$ Mg^{2+}, Na^{+}, Cl^{-}, $SO4^{2-}$, NO^{3-}) (Figure 8)

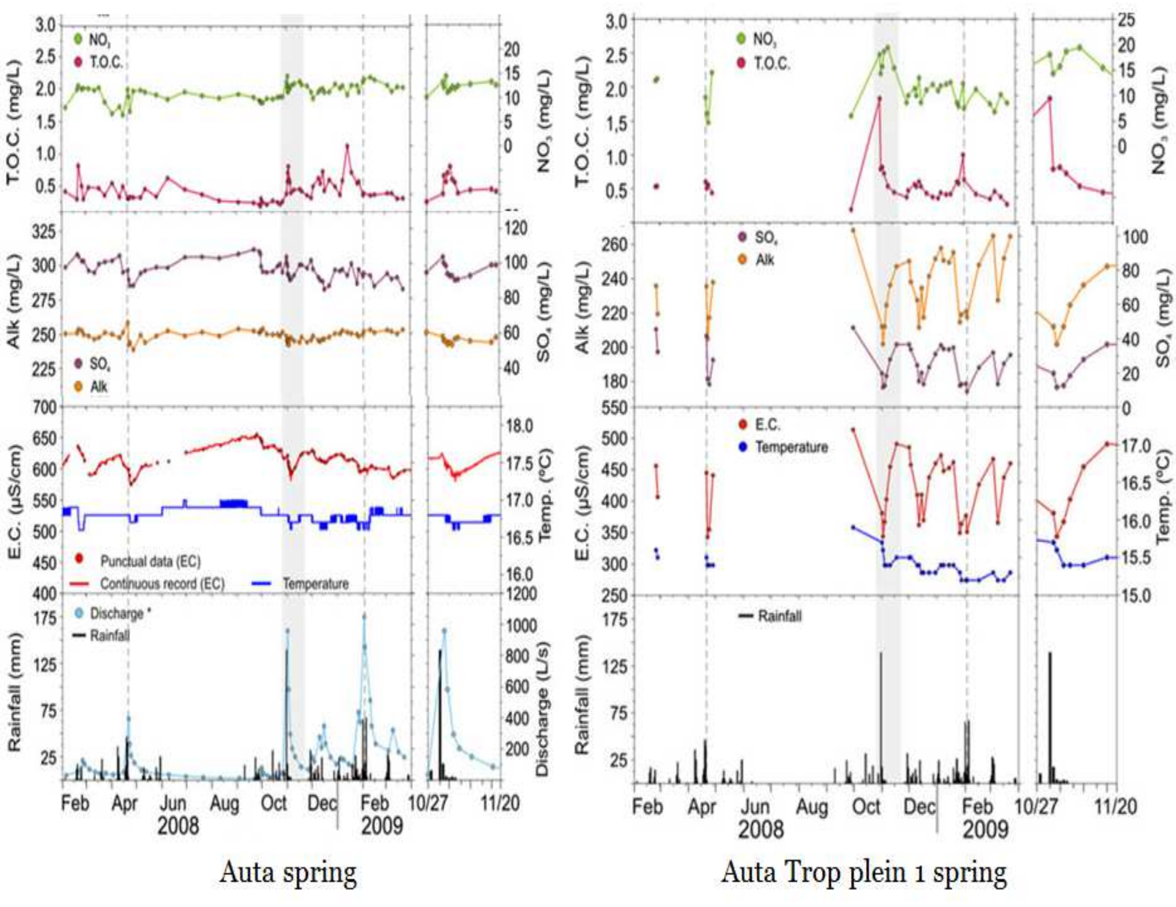

Fig 9 The hydrochemistry of Auta spring and Auta trop plein 1 (Mudarra and Andreo 2012).

The hydrochemistry of Auta and Auta Trop pleins 1 are calcium bicarbonate facies that are in concordance with the material of the aquifer although they become calcium sulphate-bicarbonate during low-water periods (Mudarra and Andreo 2012).

Figure 8 shows the variation of the chemical concentration during a rainfall event. The Auta spring is more buffered before a rainfall event and the water is more mineralized than in the Auta Trop plein 1. This is explained by the fact that Auta spring drains from the saturated zone and the water has a longer time of resident in the aquifer as a result of the lower level of karstification.

In contrary, the Auta Trop plein 1 has a faster decrease of chemical concentration during rainfall events. This spring drains namely from the unsaturated zone therefore it uses preferred conduits with a higher level of karstification (Mudarra and Andreo 2012).

5 METODOLOGHY

5.1. INTRODUCTION

A hydrological model is in general the simple representation of the reality in a computational system, considering inputs and outputs and measured values that improve to develop of the model.

The modeler should consider three basic but important elements for the development and the understanding of the hydrological model: 1) the equations that represent the behavior of the hydrological processes in the study area, for example soil storage, matrix, conduits or vadose zone, 2) the maps that helps to define the study area, recharge area, but also helps to interpret the conceptual model and modelling conceptual model, 3) the data base tables that represent the results of the numerical processes in the model, for example, precipitation, evapotranspiration and discharge data (inputs and outputs) (Chow et al.,1988).

The hydrological models are useful to measure, evaluate, manage, predict, and also discover the system hypotheses, how they function in the water resources.

5.2. MODEL SELECTION

Most hydrological systems are very complex and for the modeler it is not necessary to understand them in all details. Therefore it is necessary to understand their behavior or takes control of some parts of the models. The modeler experience helps to understand and takes control of some parts in different sort of models and can predict how is the behavior for each one.

In the study area, the lumped model was selected as was explained before, the insufficient data like topography, boreholes (to know lithology) and the small amount of data demonstrate that it couldn't be used a distributed or semi-distributed models. In this study area are known the inputs (precipitation, and discharge measurements of the Sabar River) as well as the outputs (evapotranspiration, and discharge data of the Auta spring) that all of this data help to develop several realistic assumption model and manage different possibilities of connection between the Sabar River storage and the others storage.

The lumped model was selected for easy and fast storage building also the practical connection between them in the end of the model. These practical connections generate easily other models with different assumptions but in the same approach. All the models are built with the software Matlab. The models should be as simple possible and should apply simple equations to minimize the error of procedure furthermore helping to run the model more fast.

The unknown parameters can be estimated using system identification as was described above. The experience and the literature data showed that physically based models are mathematically complex and with difficult resolutions (white box and black box) and for this reason, a simple model is desired.

5.3. MODEL DEVELOPMENT

In this study the model is built with four storages. The first storage is comprised by the soil and epikarst which together are Overflow storage. The second storage is comprised by the unsaturated zone which is Linear Reservoir storage. The third storage is comprised by the matrix and conducts (saturated zone) which together are interacting between each other and are called Linear Exchange storage. The fourth storage is comprised by the Sabar River which is river storage.

The numerical conceptual model defines different options among the storages. These possibilities manage the behavior of each of them. For the best fit in the results, the river storage is evaluated by trying to understand its participation in the karst aquifer and how it contributes to the recharge of the karst aquifer. The first possibility is to not consider the participation of the river storage (Figure 12), the second possibility is to connect the river and the aquifer with the vadose zone storage (Figure 13), the third possibility is to connect the river and the aquifer with the matrix (linear exchange storage) (Figure 14), and the fourth possibility is to connect the river and the aquifer with the conduits (linear exchange storage) (Figure 15).

The four storages are defined in the next sub chapters:

5.3.1 Overflow storage

In this study the soil and epikarst are represented by overflow storage, the water volume in this storage V_OS (t) is defined by the variations among precipitation (Auprec (t)) and real evapotranspiration (Evap_a (t)). At the time (t) the V_OS is equal to the difference between the precipitation Auprec (t) and the real evapotranspiration Evap_a (t) and the sum of volume water V_OS (t-1) of the previous time step:

$$V\_OS\ (t) = V\_OS\ (t-1) + [\ Auprec\ (t) - Evap\_a\ (t)\ ]\ \text{; (Eq.3.1)}$$

The volume V_OS (t), V_OS (t-1), Auprec (t), and Evap_a (t) are in [mm/day]. In the equation each parameter is considered unit value per [m^2]. At the end the result is multiplied by the recharge area (A) in [km^2], Evap_a (t) is the real evapotranspiration calculated for the study area (Mudarra, et al 2014).

The initial condition for V_OS (t=0) in [mm/day] is, zero:

$$V\_OS\ (0) = 0\ \text{; (Eq.3.2)}$$

The value is 0 because before the wet periods, the system is completely dry and the soil has been drained for a long time in the dry period. The real evapotranspiration (Evap_a (t)), is calculated in the following equation:

$$Evap\_a(t) = Auetp\ (t) * V\_OS(t-1)/Vmax\_OS\ \text{; (Eq.3.3)}$$

Where the Evap_a (t), Auetp (t), V_OS (t-1) and Vmax_OS are [mm/day], the value Vmax_OS is one parameter that will be calibrated with the numerical model described below (Chapter 5.4), and the value Auetp (t) is an output data.

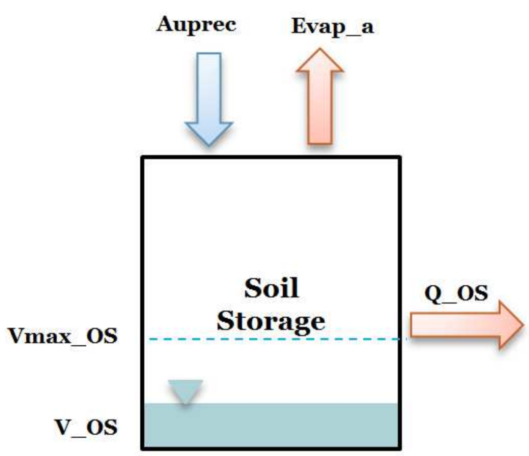

Fig 10 Soil storage representation.

The calculation of the out flow (Q_OS in [mm/day]) of the Soil storage is:

- if V_OS (t) [mm/day] is lower than 0 (V_OS(t)<0)

  Then the volume of the reservoir is: V_OS=0 [mm/day],

  and the outflow: Q_OS (t) = 0 [mm/day].

- if V_OS (t) [mm/day] > Vmax_OS [mm/day]

  Then the volume of the reservoir is: V_OS (t) = Vmax_OS

  and the outflow: Q_OS (t) = V_OS (t) - Vmax_OS [mm/day]

- if V_OS (t) [mm/day] is lower or equal to Vmax_OS [mm/day] (V_OS (t) ≤ Vmax_OS(t))

  and the outflow: Q_OS (t) = 0 [mm/day].

5.3.2 Linear reservoir storage

Linear reservoir represents by the vadose zone for in the study area, for better understanding the following equation shows simplified Darcy law:

$$Q\ (t) = -KA\frac{(h(t)-H_o)}{\Delta x}\ \text{; (Eq.3.4)}$$

Where h (t) is the water level in the aquifer and H_0 is the water level of the spring discharge, differences of both define the hydraulic slope, and Δx is the distances between h (t) and H_0 (unit of length, L), A is the cross section that the ground water flow crosses (units of length, L^2), K is the permeability or hydraulic conductivity (units of length over time, L/T). For sake of simplicity the parameters K, A, and Δx are considered constants and the final the equation is:

$$Q\ (t) = \alpha(h(t) - H_o)\ ;\ \ \alpha = -\frac{KA}{\Delta x}\ \text{; (Eq.3.5)}$$

Considering H_o = 0 and the volume storage in the aquifer is conceptualized in:

$$V\_VZ\ (t) = n * Area * h(t)\ \text{; (Eq.3.6)}$$

Where n is the effective porosity [without units] of the aquifer, and Area is the recharge area [units of length, L^2], finally h (t) is the height of the aquifer [units of length, L].

Then clearing h (t) in equations and matching, the result is:

$$V\_VZ\ (t) = K\_VZ * Q\_VZ(t)\ \ ;\ \ K\_VZ = \frac{Area*n}{\alpha};\ \text{(Eq.3.7)}$$

Where V_VZ (t) is the volume in the storage, K_VZ is a constant parameter of the vadose zone [units of time, T], Area is the represent recharge area, n the porosity, and α .

In this study, this case is considered in the following model:

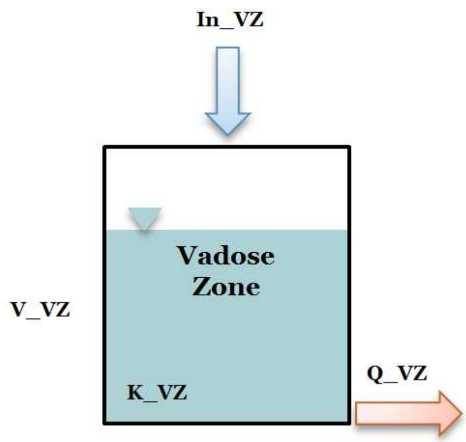

Fig 11 Vadose zone representation.

The calculation of the out flow (Q_VZ in [mm/day]) of the vadose zone is:

- If time step (i) = 1

$$\boldsymbol{Qo\_VZ = init\_VZ/\ K\_VZ};$$

- time step (i) ≥ 2

$$Qo\_VZ = V\_VZ(i-1)/\ K\_VZ;$$

Where K_VZ [days] is a parameter that will be calibrated (Chapter 5.4). init_VZ [mm/day] is the initial condition for the vadose zone and in this case will be 0. Qo_VZ [mm/day] is a flow that will be connected to other equation to calculate the complete discharge in the vadose zone. The following equation shows the discharge:

$$Q\_VZ\ (i) = in\_VZ(i) + \left(Qo\_VZ - \ in\_VZ(i)\right) * \exp(\,-1\ /\ K\_VZ\,);$$

And the volume V_VZ (i) [mm/day] is:

$$V\_VZ\ (i) = K\_VZ * Q\_VZ\ (i)\ ;$$

Where V_VZ, Q_VZ [mm/day], in_VZ is the input [mm/day], and K_VZ [day].

5.3.3 Linear exchange storage

The matrix and the conduits are represented by linear exchange storage. It assumes that the conduits with preferred flow (karst conduits) are faster in the discharge than the matrix. For this method the ground water is divided into two components. One component is the matrix and the other component is the conduits. The flow exchange is defined for difference in the water level between each other. The following equations explain this process:

$$Q_1\ (t) = \frac{V_1\ (t)}{K_1}\ ;\ \text{(Eq.3.8)}$$

Whit Q_1 (t) is flow discharge of the conduits (mm/day). V_1 is volume of the conduits [mm/day], and K_1 is a parameter represents a conduit in [days], this equation is similar to Eq.3.7, it applied the same equation of the exchange water between matrix and conduits are:

$$Q_E\ (t) = K_{12} * Area_{12} * \frac{h_2\ (t) - h_1\ (t)}{\Delta x\_12} = \frac{V_2\ (t) - f_p * V_1\ (t)}{K_E}\ ;\ \text{(Eq.3.9)}$$

Where

$$h_2\ (t) = \frac{V_2\ (t)}{A * n_2}\quad ;\quad \frac{1}{K_E} = \frac{K_{12} * Area_{12}}{A * n_2 * \Delta x_{12}}\ ;\ f_{ex} = \frac{n_2}{n_1}\ ;\ \text{(Eq.3.10)}$$

The equation above is very similar to the equation 3.4 and 3.5, K_{12} is the permeability or the hydraulic conductivity (L/T), $Area_{12}$ is the cross section where the flow crosses, Δx_{12} is the distance between flows, f_{ex} is the difference between the porosity of the matrix and the conduits ,and Q_E is the flow exchange between the reservoirs. All these parameters are considered for the hydraulic dynamic between matrixes to conduits.

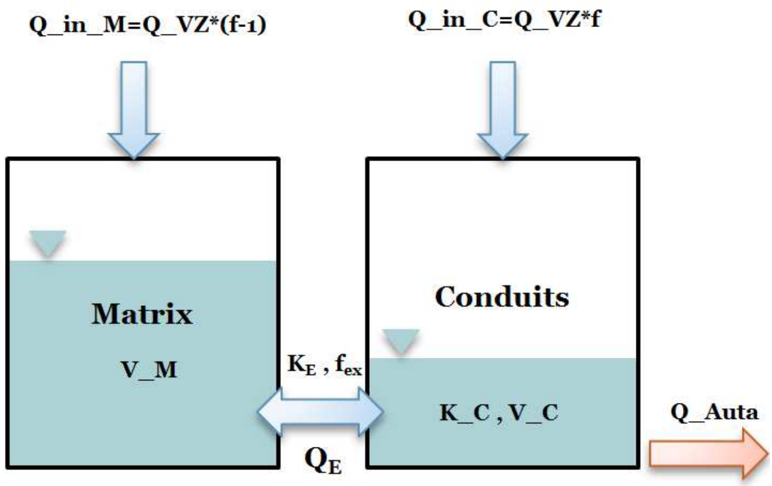

Fig 12 Matrix-Conduits exchange representation.

The following equation shows how to find that V_C and V_M. Voo_C and Voo_M [mm/day] are defined as the volumes of each storage taking into account the flow exchange between the reservoirs (matrix-conduits). Finally the Vo_C and Vo_M at (t=0) are the initial conditions for each reservoir in this case both are 0, and where (t≥1) is the volume one time step before:

$$Voo\_C = Q\_in\_C(t) + \left(\frac{(Vo\_M - f_{ex} * Vo\_C)}{K_E}\right) - \frac{Vo\_C}{K\_C}; \text{ (Eq.3.11)}$$

$$Voo\_M = Q\_in\_M(t) - \left(\frac{(Vo\_M - f_{ex} * Vo\_C)}{K_E}\right); \text{ (Eq.3.12)}$$

The Eq.3.11 and Eq.3.12 are replaced in the following equations to calculate the constants (A, B, and C), that are needed to solve the equation:

$$A_1 = -\frac{1}{2}\left(\frac{1}{K\_C} + \frac{1+f_{ex}}{K_E}\right) + \sqrt{\left(\frac{1}{4} + \frac{(1+f_{ex})}{K_E}\right)^2 - \frac{1}{K\_C * K_E}}; \text{(Eq.3.13)}$$

$$A_2 = -\frac{1}{2}\left(\frac{1}{K\_C} + \frac{1+f_{ex}}{K_E}\right) - \sqrt{\left(\frac{1}{4} + \frac{(1+f_{ex})}{K_E}\right)^2 - \frac{1}{K\_C * K_E}}; \text{(Eq.3.14)}$$

$$C_1 = K\_C * (Q\_in\_M(t) + Q\_in\_C(t)) \text{ ;(Eq.3.15)}$$

$$C_2 = K_E \ * Q_{in\_M(t)} + K\_C * f_{ex}(Q\_in\_M(t) + Q\_in\_C(t)) \text{ ;(Eq.3.16)}$$

$$B_1 = \frac{(Voo\_C - (A_2 * Vo\_C) + (A_2 + C_1)}{A_1 - A_2} \text{ ;(Eq.3.17)}$$

$$B_2 = (Vo\_C - B_1 - C_1) \text{ ;(Eq.3.18)}$$

$$B_3 = \frac{(Voo\_M - (A_2 * Vo\_M) + (A_2 + C_2)}{A_1 - A_2} \text{ ;(Eq.3.19)}$$

$$B_4 = (Vo\_M - B_3 - C_2) \text{ ;(Eq.3.20)}$$

Where K_C, K_E and f_{ex} are parameters that are calibrated and validated in the process explained bellow (Chapter 5.4). The resulting equations for V_C and V_M are:

$$V\_C(t) = B_1 * \exp(A_1) + B_2 * \exp(A_2) + C_1 \text{;(Eq.3.21)}$$

$$V\_M(t) = B_3 * \exp(A_1) + B_4 * \exp(A_2) + C_2 \text{;(Eq.3.22)}$$

Finally the value V_C (t) and V_M (t) (Eq.3.21, Eq.3.22) are replaced in the Eq.3.23 and Eq.3.24, where the results are:

$$Q_E(t) = \frac{V\_M\,(t) - (f_{ex} * V\_C\,(t))}{K_E} \text{;(Eq.3.23)}$$

$$Q\_Auta(t) = \frac{V\_C\,(t)}{K\_C} \text{;(Eq.3.24)}$$

Where the results Q_E is the flow exchange between reservoirs in [mm/day], and Q_Auta is the modelled discharge in [mm/day], K_E and K_C in [days], V_M and V_C are in [mm/day].

5.3.4 River storage

The river is represented by River storage. This storage is the Sabar River and only the partial flow is going to the aquifer and the other part is going to downstream. The following equation explains this process:

$$Q\_river(t) = Aurvier(t) * friver \text{ ; (Eq.3.25)}$$

Where the result Q_river is [mm/day], Aurvier [m^3/sec] and friver [between 0 and 1]

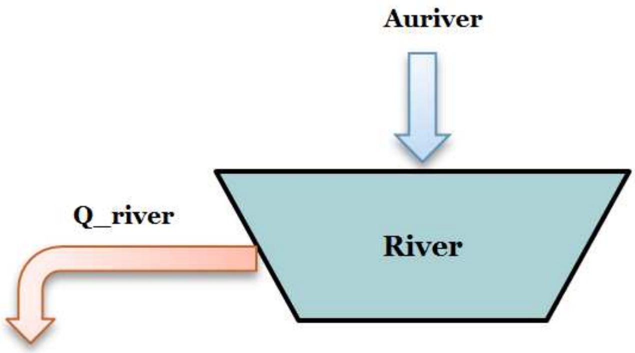

Fig 13 River storage representation.

Q_river (t) is the discharge of the river storage that is going to the aquifer. Furthermore it is joined as a input with the other storages, the following chapter shows.

5.4 MODEL DESCRIPTION

In this chapter, the four numerical conceptual models used in this study will be described.

5.4.1 Exchange model

In this model the overflow storage is first represented as the soil storage and the epikarst, where the water flows across the overflow storage to the vadose zone represented as linear reservoir storage. Secondly the discharge from the vadose zone is divided into the matrix and conduits, where the discharge is multiply by a factor f (between 0-1), and one part is going to the conduits and other to the matrix. In the third step, the linear exchange storage represents the flow exchange between the matrix and conduits. Finally the output of the chain of linear exchange storage is the modelled discharge of Auta spring (Q_Auta) (Figure 13).

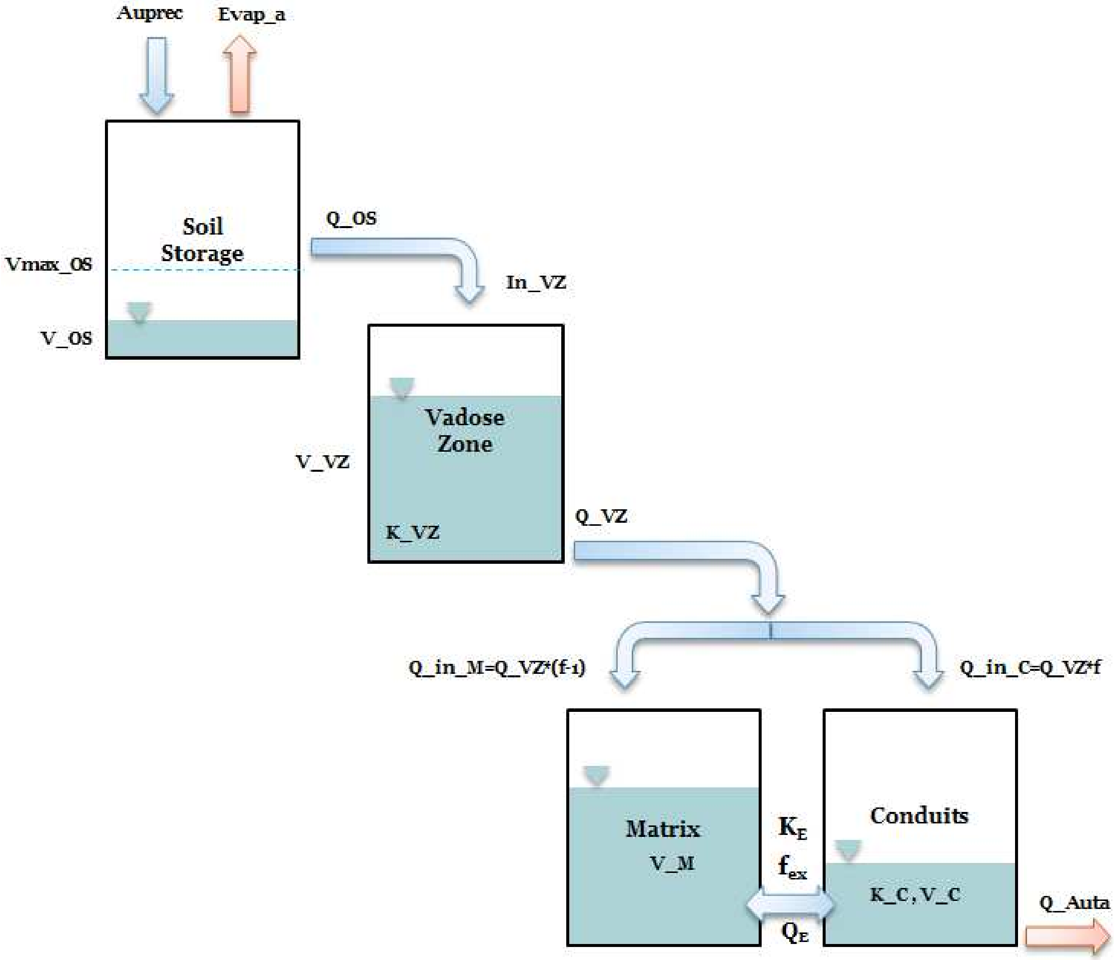

Fig 14 Exchange model representation.

The parameters values can be found in the appendix A1, and the model code in the appendix A2.

The precipitation is recharged the soil storage (chapter 5.3.1), the discharge corresponds to:

Q_OS [mm/day] = in_VZ [mm/day];

The outflow of the soil storage Q_OS [mm/day] is the input to the vadose zone in_VZ [mm/day], and the vadose zone discharges is:

Q_VZ [mm/day] = Q_in_M + Q_in_C [mm/day];

Q_in_M= Q_VZ *(1-f);

Q_in_C = Q_VZ *f; f [0-1]

The discharge flow of the vadose zone Q_VZ [mm/day] is multiplied by the factor f and is separate in two flows and one of them is the input to the matrix and the other to the conduits Q_in_M and Q_in_C [mm/day] (linear exchange storage, chapter 5.3.3), and finally the linear exchange (Matrix-conduits) discharges is the modelled flow (Q_Auta [mm/day]).

5.4.2 Exchange-river-vadose zone model

In this model is the same representation of the exchange model in except the influence of river discharge, part of the river discharge is multiplied by a factor friver (between 0-1), and is joined to the discharge of the overflow storage. The sum of both is the input to the vadose zone, then the process continuous normally. Finally the discharge of the linear exchange storage is the modelled discharge of Auta spring (Q_Auta) (Figure 14).

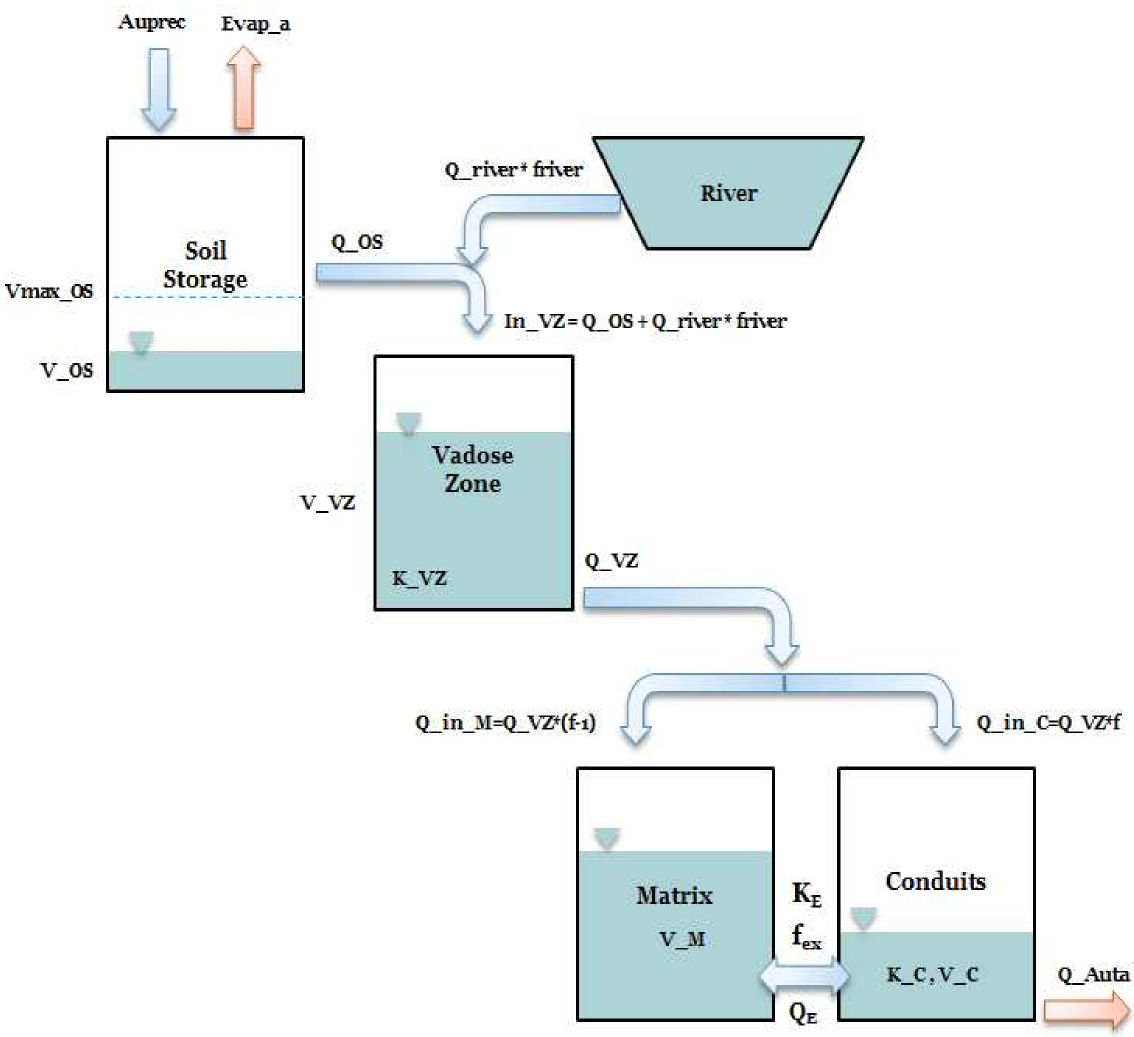

Fig 15 Exchange-river-vadose zone model representation.

The parameters values can be found in the appendix A1, and the model code in the appendix A2.

The precipitation is recharged the soil storage (chapter 5.3.1), the discharge corresponds to:

Q_OS [mm/day] + Q_river [m^3/sec] * friver [0-1] = in_VZ [mm/day];

The outflow of the soil storage Q_OS [mm/day] and Qriver [m^3/sec] are the input for the vadose zone in_VZ [mm/day], and the discharge for the vadose zone is:

Q_VZ [mm/day] = Q_in_M + Q_in_C [mm/day];

Q_in_M= Q_VZ *(1-f);

Q_in_C = Q_VZ *f; f [0-1]

The discharge flow of the vadose zone Q_VZ [mm/day] is multiplied by a factor f and is separate in two flows and one of them is the input for the matrix and the other for the conduits Q_in_M and Q_in_C [mm/day] (linear exchange storage, chapter 5.3.3) and finally the discharge for the linear exchange (matrix-conduits) is the modelled discharge (Q_Auta [mm/day]).

5.4.3 Exchange-river-matrix model

In this model is the same representation of the exchange model in except the influence of river discharge, part of the river discharge is multiplied by a factor friver (between 0-1) and is joined to the discharge of the vadose zone. The discharge of the vadose zone is multiplied by another factor f (between 0-1), where is divided in two flows. One of them is going to the matrix and the other to the conduits (Q_in_M and Q_in_C). The flow of the river is joined to the flow is coming to the matrix and both are inputs for one part of the linear exchange storage which is the matrix part. Finally the discharge of the linear exchange storage is the modelled discharge of Auta spring (Q_Auta) (Figure 15).

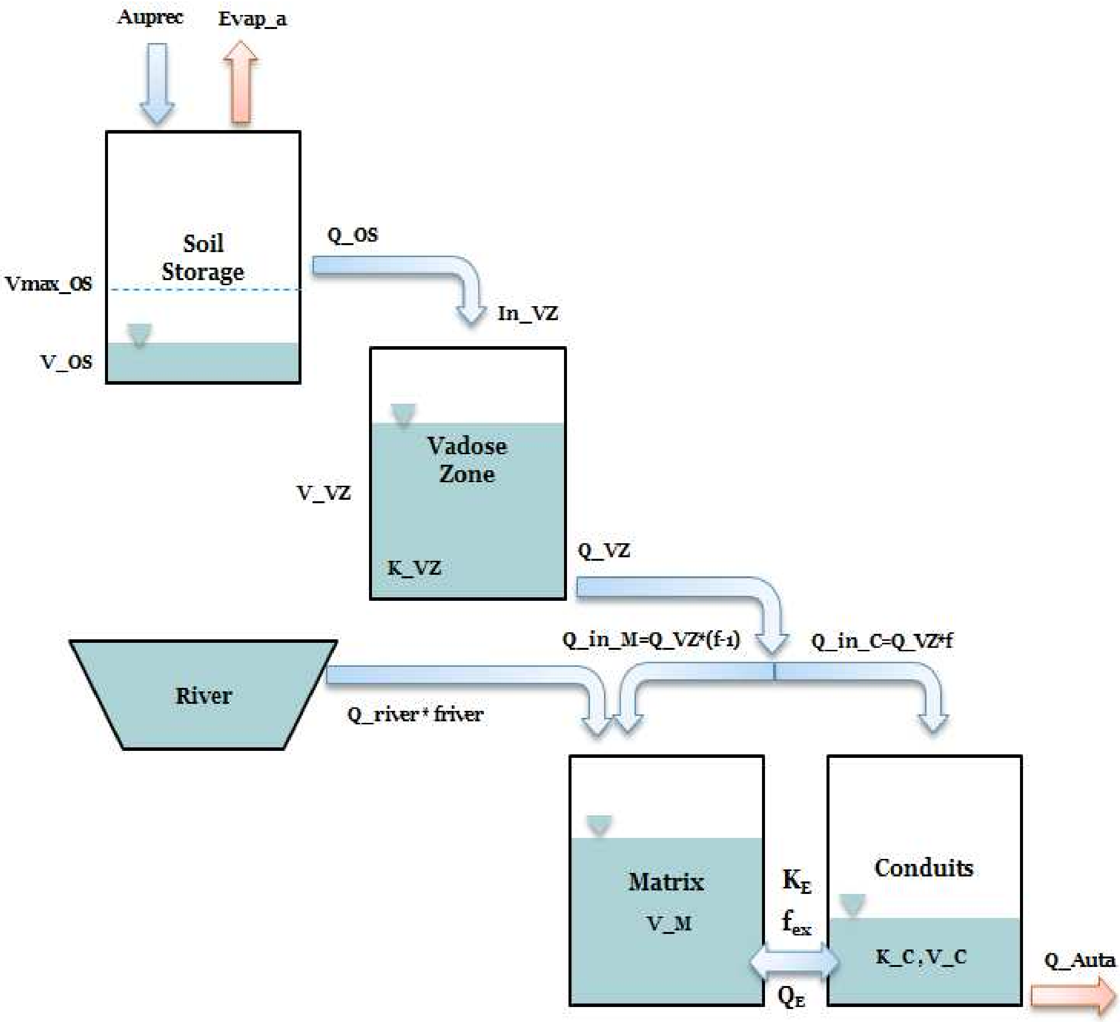

Fig 16 Exchange-river-matrix model representation.

The parameters values can be found in the appendix A1, and the model code in the appendix A2.

The precipitation is recharged the soil storage (chapter 5.3.1), the discharge corresponds to:

Q_OS [mm/day] = in_VZ [mm/day];

The outflow of the soil storage Q_OS [mm/day] is the input for the vadose zone in_VZ [mm/day], and the discharge for the vadose zone is:

Q_VZ [mm/day] = Q_in_M + Q_in_C; [mm/day]

Q_in_M= Q_VZ *(1-f) +Q_river [m^3/sec] * friver; friver [0-1]

Q_in_C = Q_VZ *f; f [0-1]

The discharge of the vadose zone Q_VZ [mm/day] is multiplied by the factor f and is separate in two flows and one of them is the input for the matrix and the other for the conduits (Q_in_M and Q_in_C [mm/day]) (linear exchange storage, chapter 5.3.3) and the river discharge is joined to the flow is going to the matrix. Finally the discharge for the linear exchange storage (matrix-conduits) is the modelled discharge (Q_Auta [mm/day]).

5.4.4 Exchange-river-conduits model

In this model is the same representation of the exchange model in except the influence of river discharge, part of the river discharge is multiplied by a factor friver (between 0-1) and is joined to the discharge of the vadose zone. The discharge of the vadose zone is multiply by another factor f (between 0-1), where is divide in two flows one of them is going to the matrix and the other to the conduits (Q_in_M and Q_in_C), the flow of the river is joined to the flow is coming to the conduits and both are inputs for one part of the linear exchange storage which is the conduits part. Finally the discharge is the modelled discharge of Auta spring (Q_Auta) (Figure 16).

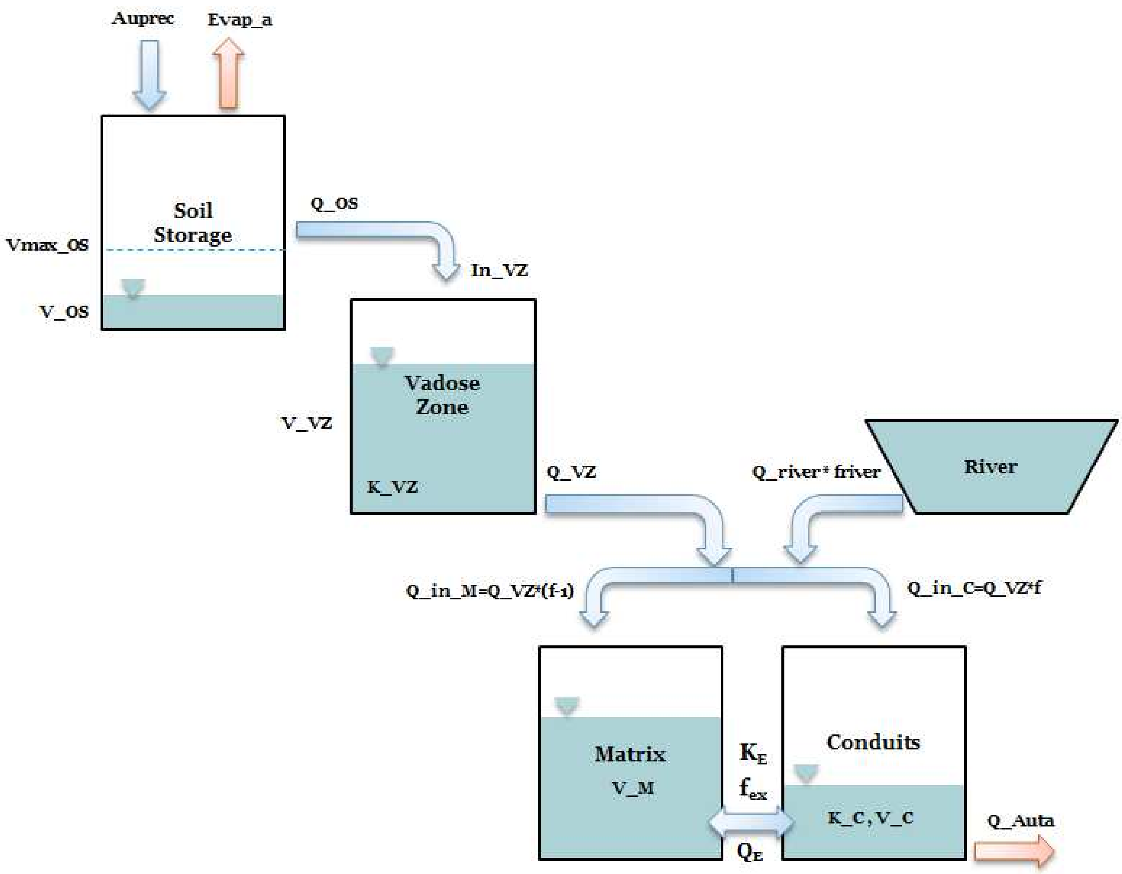

Fig 17 Exchange-river-conduits model representation.

The parameters values can be found in the appendix A1, and the model code in the appendix A2.

The precipitation is recharged the soil storage (chapter 5.3.1), the discharge corresponds to:

Q_OS [mm/day] = in_VZ [mm/day];

The outflow of the soil storage Q_OS [mm/day] is the input for the vadose zone in_VZ [mm/day], and the discharge for the vadose zone is:

Q_VZ [mm/day] = Q_in_M + Q_in_C; [mm/day]

Q_in_M= Q_VZ *(1-f); f [0-1]

Q_in_C = Q_VZ *f+ Q_river [m^3/sec] * friver; friver [0-1]

The discharge flow of the vadose zone Q_VZ [mm/day] is multiplied by the factor f and is separate in two flows and one of them is the input for the matrix and the other for the conduits (Q_in_M and Q_in_C [mm/day]) (linear exchange storage, chapter 5.3.3) and the river discharge is joined to the flow is going to the conduits, finally the discharge for the linear exchange storage (matrix-conduits) is the modelled discharge (Q_Auta [mm/day]).

6 MODEL CALIBRATION

In this part of the study is to define the best fit of the parameters therefore obtaining the good proximity with the reality. One method with excellent results is the shuffled complex evolution (SCE) method developed at the University of Arizona (Duan et al., 1992).

6.1 THE SHUFFLED COMPLEX EVOLUTION (SCE-UA)

The SCE-UA method was developed at the University of Arizona. The method is a general purpose of global optimization algorithm. The SCE-UA applies a combination of different methodologies that are four, a) random search, b) evolution of communities, c) the simplex method, and d) complex shuffling.

The sample points constitute a population and the population are partitioned in several communities (complexes) each consisting of 2n + 1 points, where n is the number of parameters to be optimized , and then each community evolve independently of the others, this evolution depends of the search range and initial value. The search range is defined by maximum and minimum values that need to be into the reality, the initial value is located within the search range, the research value and initial value is defined by the modeler according experience or existing literature, after certain period of increment , the communities are forced to mix it and then new communities are formed through a process of shuffling, the evolution and shuffling steps repeat until convergence criteria are satisfied (detailed explanation of the method is given in Duan et al. (1992, 1993, 1994).

The SCE-UA method has been applied to hydrologist and hydrogeologist models obtaining results efficiently and automatically.

For this study, the shuffled complex evolution or automatic calibration shows the better numerical fit for each model but not consider the realistic results that it will be evaluate for the modeler.

7 MODEL EVALUATION

7.1 NASH SUTCLIFFE EFFICIENCY (NSE)

The Nash-Sutcliffe efficiency was proposed by Nash and Sutcliffe (1970) is the method most widely used for calibration and validation of hydrological models and in this study is used in karstic hydrogeological model with observed data.

The Nash-Sutcliffe efficiency is defined by one minus the sum of the absolute square and difference between observed discharge and simulated discharge and divided of the sum of the absolute square and difference between observed discharge and the mean of observed discharges.

The Nash–Sutcliffe model efficiency coefficient is defined as:

$$\mathrm{NSE} = 1 - \left[\frac{\sum_{t=1}^{n}[Q_{obs}(t)-Q_{sim}(t)]^2}{\sum_{t=1}^{n}[Q_{obs}(\mathrm{t})-\overline{Q_m}]^2}\right]; \text{Eq.5.1}$$

Where Q_{obs} is observed discharge at time (t), and Q_{sim} is simulated discharge at the time (t), and Q_m is the mean of observed discharge.

The NSE ranges between -∞ and 1, when is 1, it means that the model is perfect with optimal value, when is between 0 and 1, it is a range of performance when it is more close to 1 is better than to be close to 0, when is ≤0, it means the mean of observed discharge is better predictor than the simulated discharge that is unacceptable.

7.2 MONTE CARLO SAMPLING-SENSITIVITY ANALYSIS

The Monte Carlo Sampling is based techniques are often applied for the estimation of uncertainties in hydrological models due to uncertain parameters, this technique is repeat randomly different parameters of the model and obtain numerical results.

In the following, it shows the methodology for Monte Carlo Sampling:

- Select the inputs model imprecisely without knowledge of the reality, it is to try to define a purpose the inputs and identify the parameters that has significant impact in the output also it helps to eliminate the redundant uncertain inputs.

- Assign the visual threshold and probability distribution for each parameter.

- Generate many parameter set randomly with their respective model result, it requires to select an appropriate parameter set scheme, the most common choose is Monte Carlo Sampling.

- Run the model for all the parameter set and estimate the uncertainty in the model outputs, it should be ensure that enough simulation has been performed to have the outputs and stable solutions.

Monte Carlo sampling also works in the beginning pretty closes that the shuffled complex evolution, but in this case Monte Carlo sampling make iterations and the modeler can choose how many iterations it will be better for the model, in this case it was ten thousands (10,000) iterations per parameter calibrated. Monte Carlo sampling is based in the sensitivity analysis. The shape of the iterations shows the sensitivity of each parameter (Figure 17).

In this study, sensitivity analysis is applied as an instrument for the assessment of the input parameters with respect to their impact on model outputs, and it is useful not only for model development, but also for model validation and reduction of uncertainty.

Sensitivity analyst is a mathematical procedure that uses probability distribution, the probability distribution works with the uncertainty in the input data, every input data has a visual threshold of uncertainty in view of measuring issues, accessibility, environmental pollution or external agent to influence in the outcomes of the model. Sensitivity analyst is valuable tool to identify which parameters are sensitive with respect at the observation data, some parameters can be more sensitive than the others, and insensitive parameter helps to understand the conceptual model also identifying which parameter is useless or not necessary in the model, in other hand that the parameters seem to be insensitive may have important relationship (direct correlation) with other parameter and are essential for the conceptual model.

The sensitivity analysis has a sensitive function, is a curve that describe how sensitive is the parameter or not, it shows (Appendix A3)

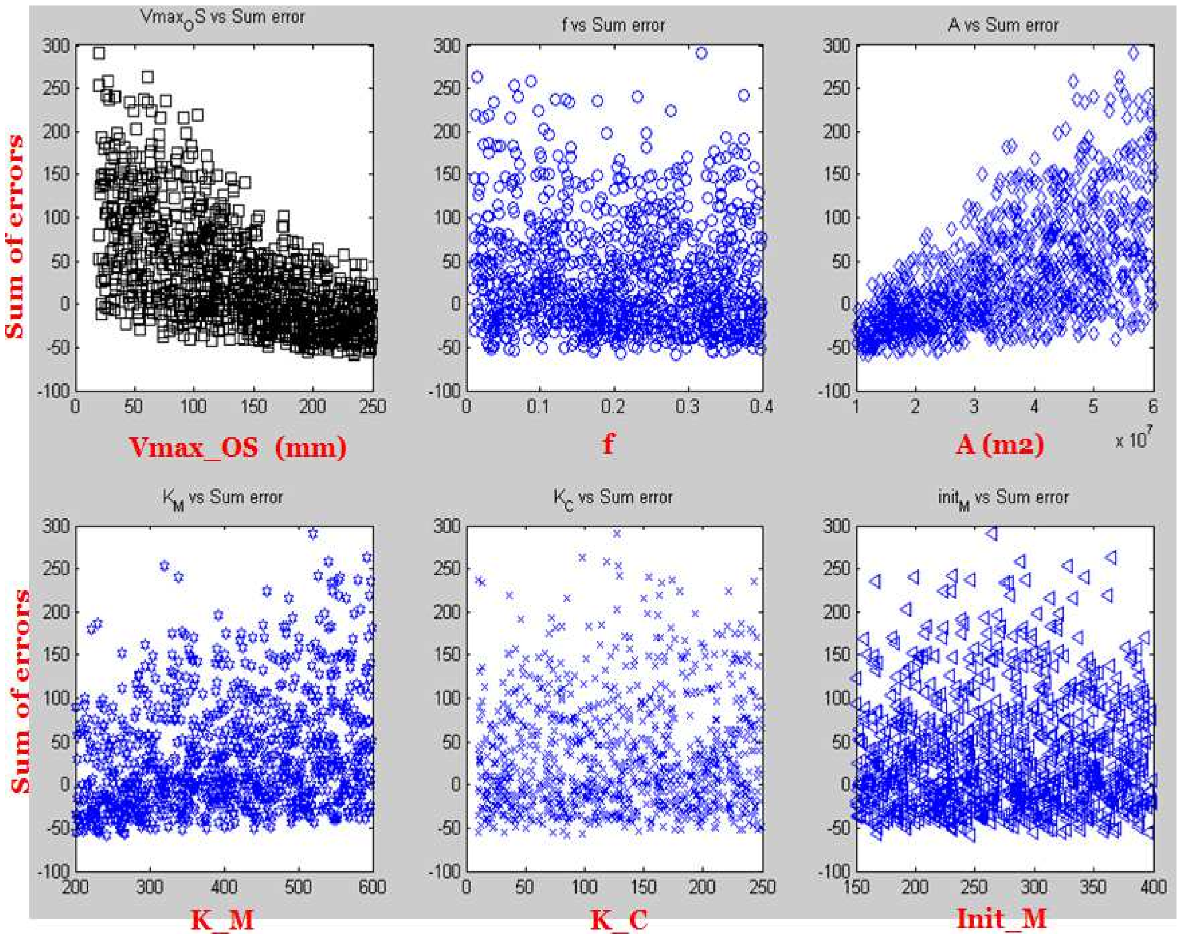

Fig 18 Sensitivity analyst and Monte Carlo sampling for each parameter.

In the following, sensitive analyst has often reason to be applying:

- Evaluation a big amount of results data (outcomes)

- Increasing to understand the relationship among inputs and outputs in the numerical model.

- Reduction of uncertainty, identifying the inputs may cause a significant uncertainty in the output data, these problems should be focus of attention.

- Model simplification, fixing the model that no has effect in the results probably deleting or replacing data.

7.3 RECHARGE RATE

The recharge rate is the percentage of water infiltration that crosses all the systems until the outlet with respect to the input; the output could be simulated data, measured data or observation data and the input is the precipitation.

The recharge rate is calculated as follow (Eq. 5.2):

$$RR\% = \frac{Output}{Input} * 100 \text{ ; Eq. 5.2}$$

Where Output [mm/day] is the modeled data, input [mm/day] is the precipitation; both of the values need to be in the same unit.

For the karst aquifer the recharge rate between 45% and 55% the value is realistic and within acceptable interval, if the recharge rate is >55% the value is unrealistic, see the appendix A4 for more information.

8 RESULTS

8.1 AUTOMATIC CALIBRATION BY THE SHUFFLED COMPLEX EVOLUTION (SCE-UA) AND NASCH SUTCLIFFE EFFICIENCY (NSE).

Four models were run with the data available and it was applied the Shuffled Complex Evolution (SCE-UA) and Nash Sutcliffe Efficiency (NSE) for each model.

The following graphics (figure 18-21) show the precipitation in [mm/day], Auta discharge or observation data in [l/s] and modelled data in [l/s]. The modelled data is the result of each model after several mathematical processes.

The table below (table 2-5) shows the numbers of parameters were used in each model also the visual threshold for each parameters (Lower bound and Upper bound) that it was defined for the modeler with experience or literature information. Furthermore the automatic calibration (SCE-UA) shows the optimal set, it means the best automatic fit for each parameter. Finally the last part of the graphic shows the Nash Sutcliffe Efficiency (NSE). If NSE is more close to 1, the optimal set are better or it has better fit comparing to the observation data. The modeler needs to evaluate the results are realistic or do not.

In the table 6, shows the summary of parameters and Nash Sutcliffe Efficiency (NSE) for each model, the efficiency of the all the models are very close between each other.

a) Exchange model

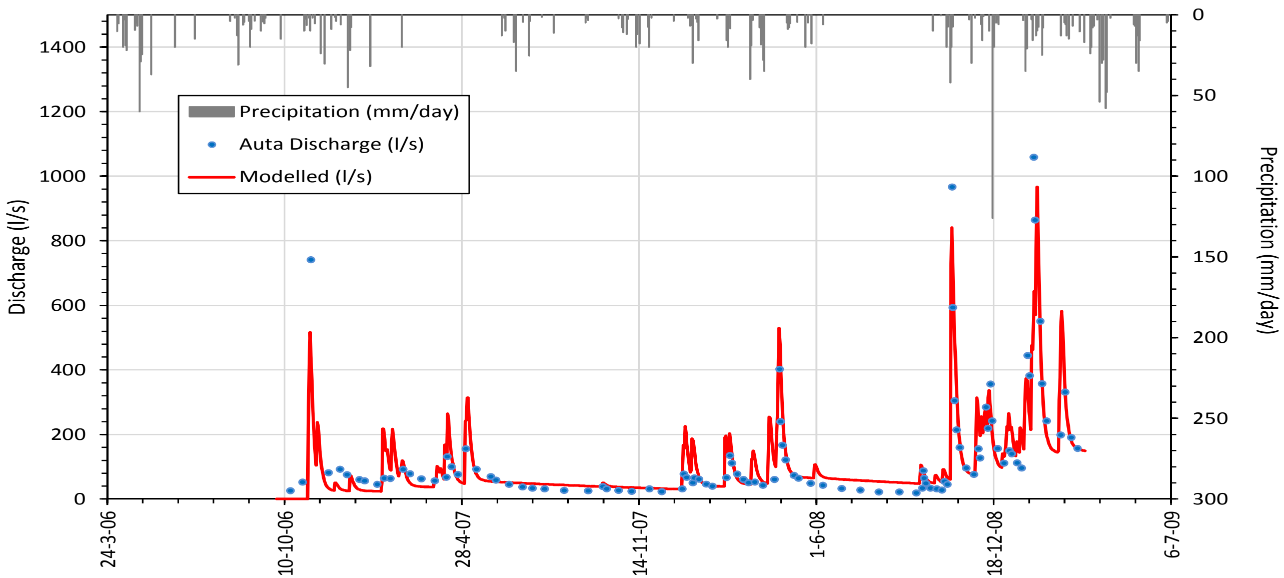

Fig 19 Exchange model results Observation-Modelled data.

Model Name	Model	Parameters						Nash sutcliffe efficiency (NSE)
		Vmax_OS [mm]	K_VZ [days]	f [-]	K_C [days]	K_ex [days]	fex	
Exchange model	Optimal set	87.6034	3.5850	1.0000	2.6091	105.0942	99.9987	0.7767
	Lower bound	0	1	0	1	50	1	
	Upper bound	250	15	1	30	250	100	

Table 2 Exchange model parameters and NSE.

b) Exchange river-vadose zone model

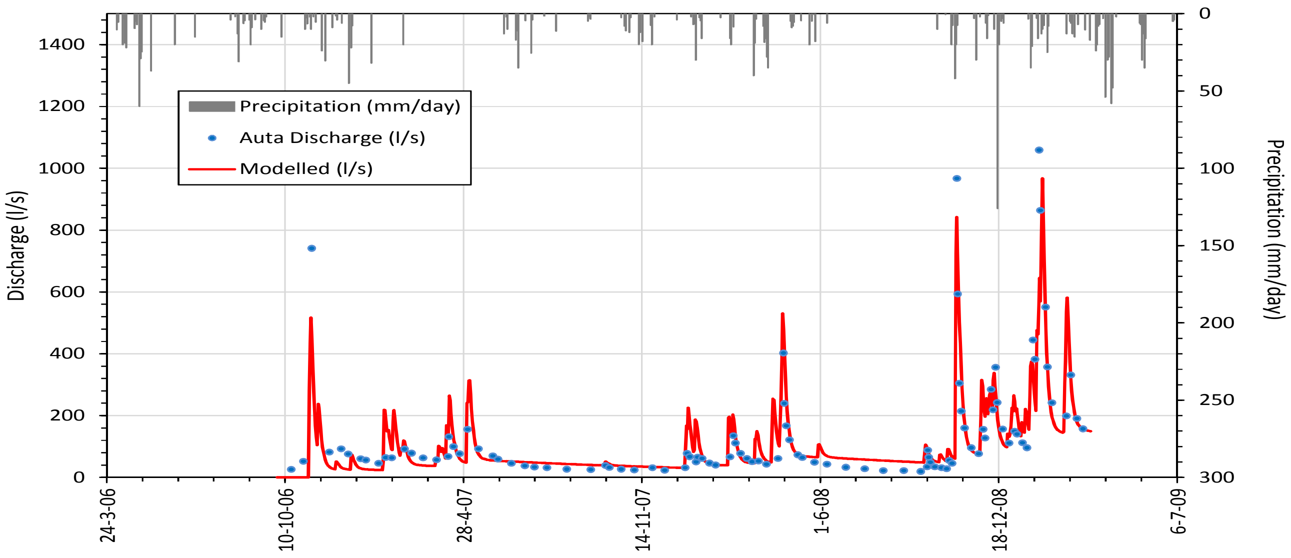

Fig 20 Exchange river-vadose zone model results Observation-Modelled data.

Model Name	Model	Parameters							Nash sutcliffe efficiency (NSE)
		Vmax_OS [mm]	friver[days]	K_VZ [days]	f [-]	K_C [days]	K_ex [days]	fex	
Exchange river-vadose zone model	Optimal set	87.6480	2.463E-06	3.5799	0.9999	2.6081	105.0921	99.9963	0.7767
	Lower bound	0	0	1	0	1	50	1	
	Upper bound	250	1	15	1	30	250	100	

Table 3 Exchange-river-vadose zone model parameters and NSE.

c) Exchange river-matrix model

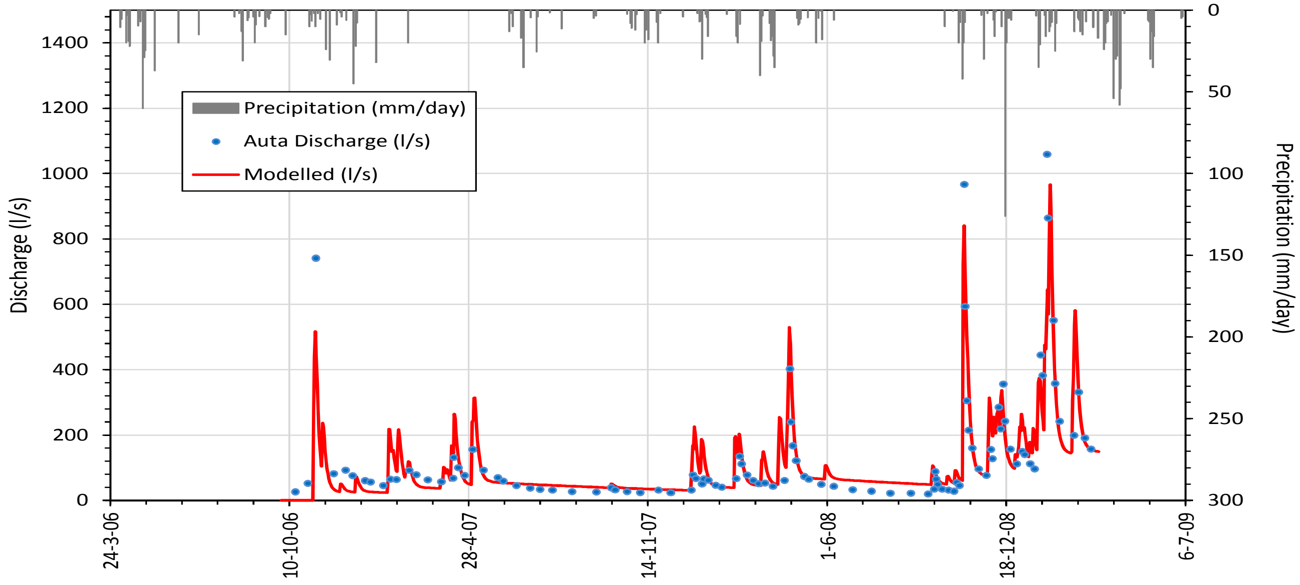

Fig 21 Exchange river-matrix model results Observation-Modelled data.

Model Name	Model	Parameters							Nash sutcliffe efficiency (NSE)
		Vmax_OS [mm]	friver[days]	K_VZ [days]	f [-]	K_C [days]	K_ex [days]	fex	
Exchange river-matrix model	Optimal set	87.5077	8.089E-06	3.5828	0.999993	2.6162	105.4145	99.9992	0.7767
	Lower bound	0	0	1	0	1	50	1	
	Upper bound	250	1	15	1	30	250	100	

Table 4 Exchange river-matrix model parameters and NSE.

d) Exchange river-conduits model

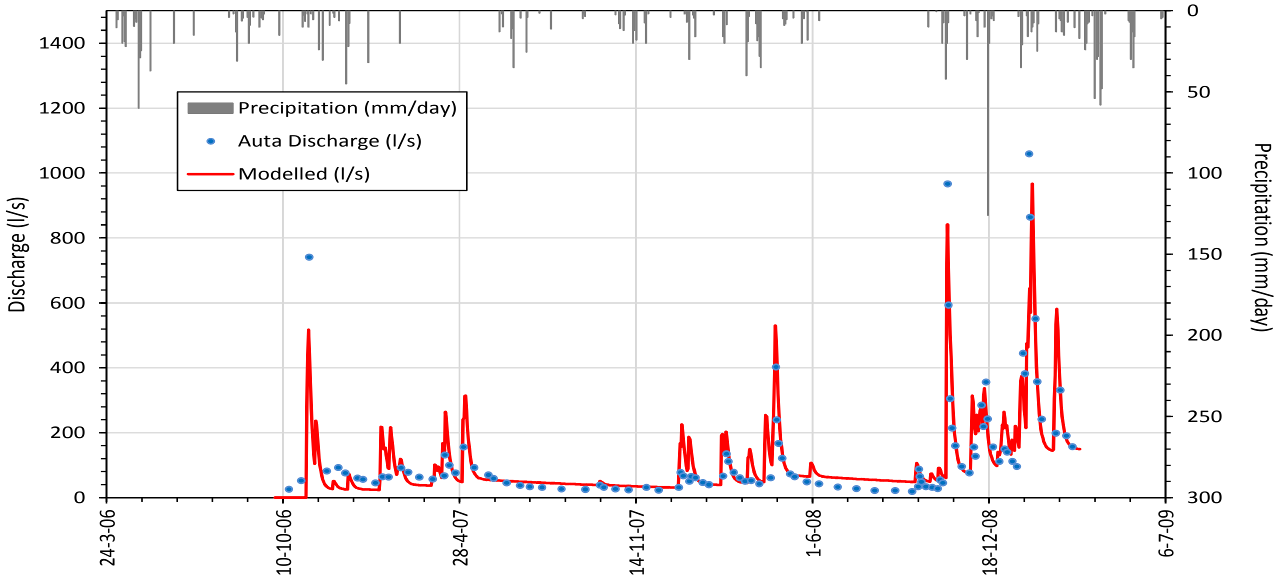

Fig 22 Exchange river-conduits model results Observation-Modelled data.

Model Name	Model	Parameters							Nash sutcliffe efficiency (NSE)
		Vmax_OS [mm]	friver[days]	K_VZ [days]	f [-]	K_C [days]	K_ex [days]	fex	
Exchange river-conduits model	Optimal set	87.4976	9.685E-06	3.5841	0.99982	2.6191	105.6596	99.9905	0.7767
	Lower bound	0	0	1	0	1	30	1	
	Upper bound	250	1	15	1	30	250	100	

Table 5 Exchange river-conduits model parameters and NSE.

Model	Number of parameters	Nash sutcliffe efficiency (NSE)
Exchange model	6	0.77669969
Exchange river-vadose zone model	7	0.77669866
Exchange river-matrix model	7	0.77669916
Exchange river-conduits model	7	0.77669755

Table 6 Summary of the parameters and Nash Sutcliffe Efficiency (NSE).

8.2 MONTE CARLO SAMPLING RESULTS

The Monte Carlo sampling shows the number of iterations versus Nash Sutcliffe efficiency (NSE, which is 1-ns). In this case, the greatest fit value should be close to 0 that it shows Figure 24-27. The purple point means the best fit into the ten thousands iterations.

In the figure 22 shows that the shape of the points cloud has a uniform distribution. It means that the one value of ns is having many different possibilities within a visual threshold between 0 and 1 (axis friver).

In the figure 23 shows the shape of the points cloud are not uniform. It means that the one value with best fit is in ns between 0.2 and 0.4 approximately but having a few possibilities in the visual threshold among 0 and 7 approximately (axis K_C). It has better fit, and few visual thresholds that improve the parameter value.

In the appendix A3 shows all the Sensitive Analysis grapichs. It is evaluated all the parameters for each model.

In the graphics (Figure 24-27) shows the relations between the shape of the points cloud and the sensitivity, and the majority of the models have a greatest sensitivity in the parameters K_VZ, f, and K_C. It can distinguish seeing the shape of the point clouds. While the shape are not uniform is more sensitive. Where K_VZ [days] is a constant parameter of the vadose zone, f [between 0-1] is the division flow factor that it is applied of the vadose zone discharge. Finally K_C [days] is a constant parameter of the conduits.

In the other case, the parameters Vmax_OS, friver, K_E, and f_{ex} have a less sensitivity in the parameters, where Vmax_OS [mm/day] is a maximum volume in the soil storage. Friver [between 0-1] is the division flow factor that it is applied in the river discharge, K_E [days] is an exchange constant between the matrix and the conduits. Finally f_{ex} [days] is the division between the matrix porosity and the conduits porosity that it is explained in the linear exchange storage.

The parameter friver in the Exchange river-vadose zone model and the Exchange river-conduits model have a less sensitivity than the Exchange river-matrix model however the difference is minimum.

The parameter Vmax_OS, f_{ex}, and K_E have the same sensitivity in all the four models.

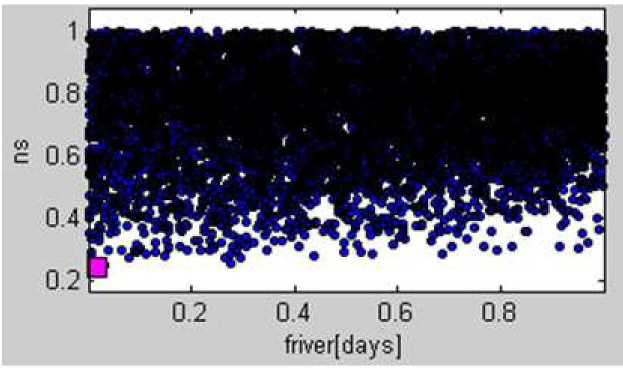

Fig 23 Monte Carlo sampling (10000 iterations), Parameter friver.

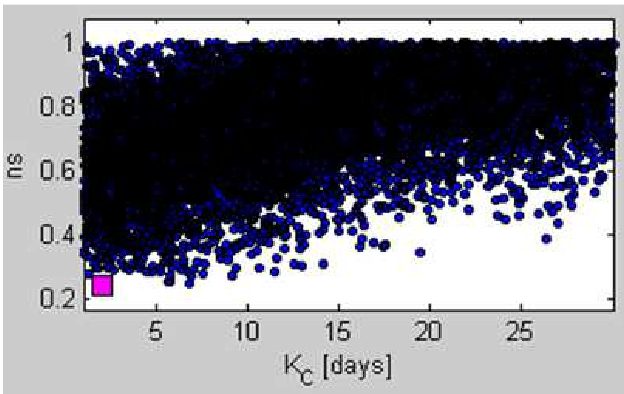

Fig 24 Monte Carlo sampling (10000 iterations), Parameter K_C.

a) **Exchange model**

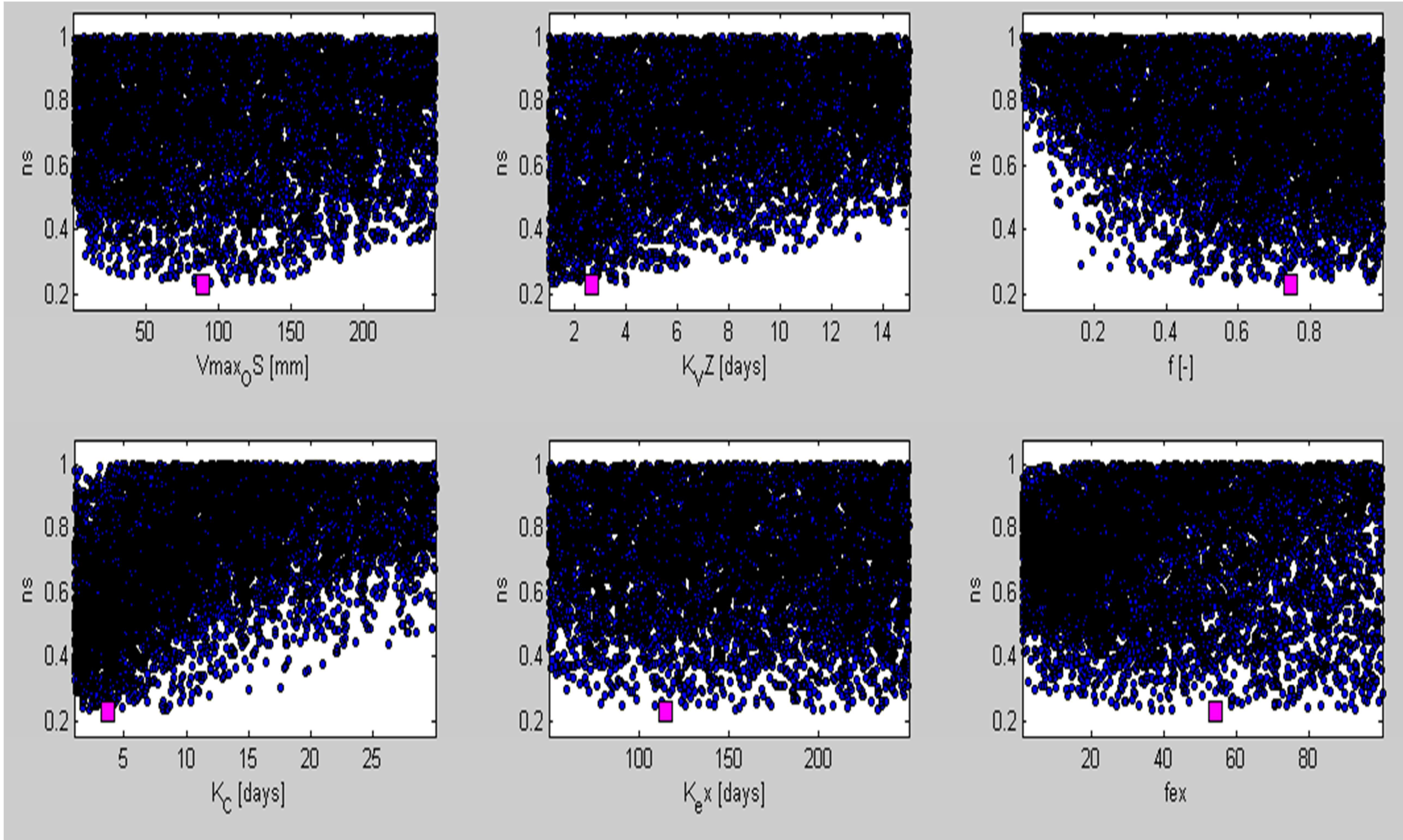

Fig 25 Exchange model, 10000 iterations pear parameter and relative sensitivity functions.

b) Exchange river-vadose zone model

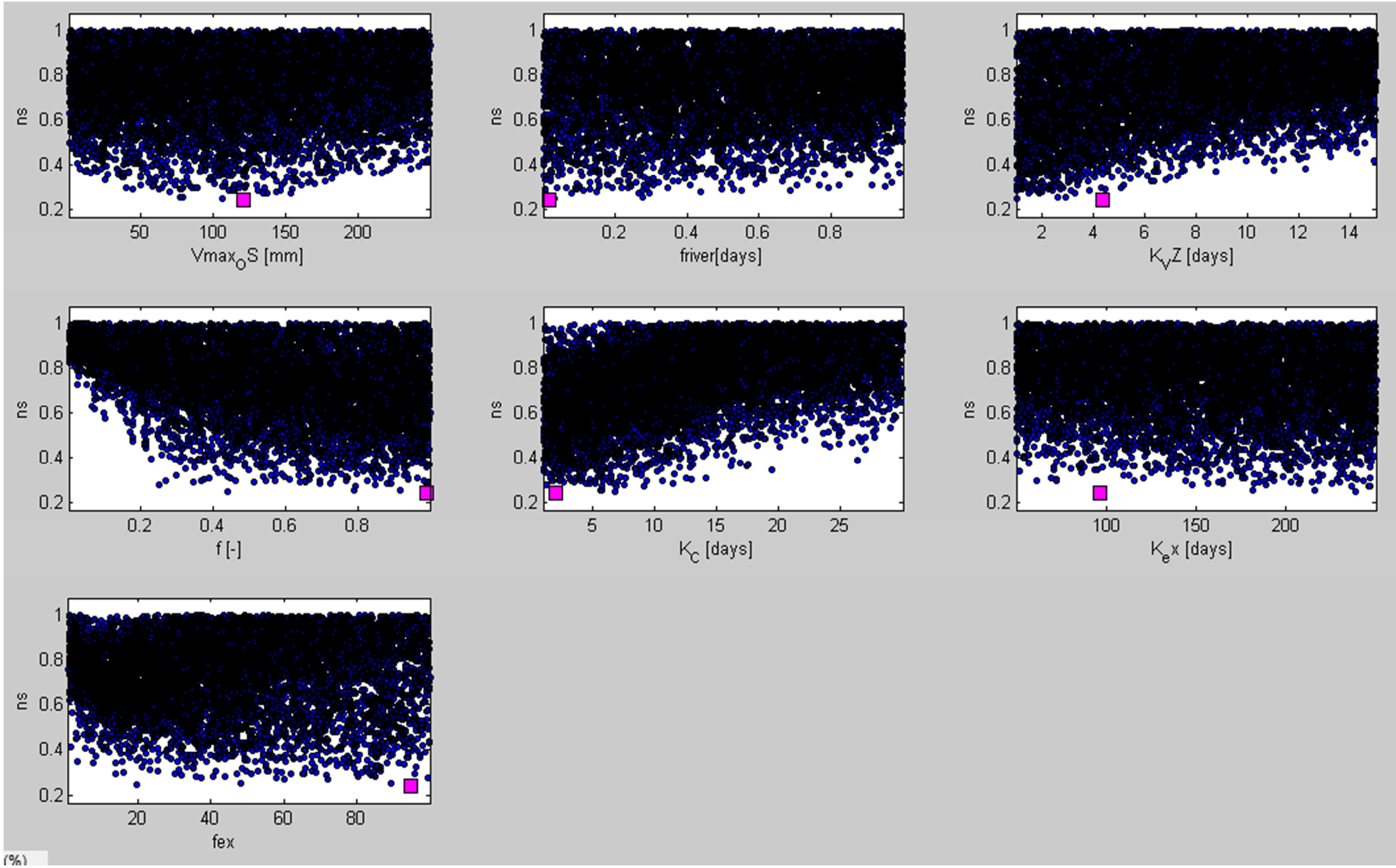

Fig 26 Exchange river-vadose zone model, 10000 iterations pear parameter and relative sensitivity functions.

c) <u>Exchange river-matrix model</u>

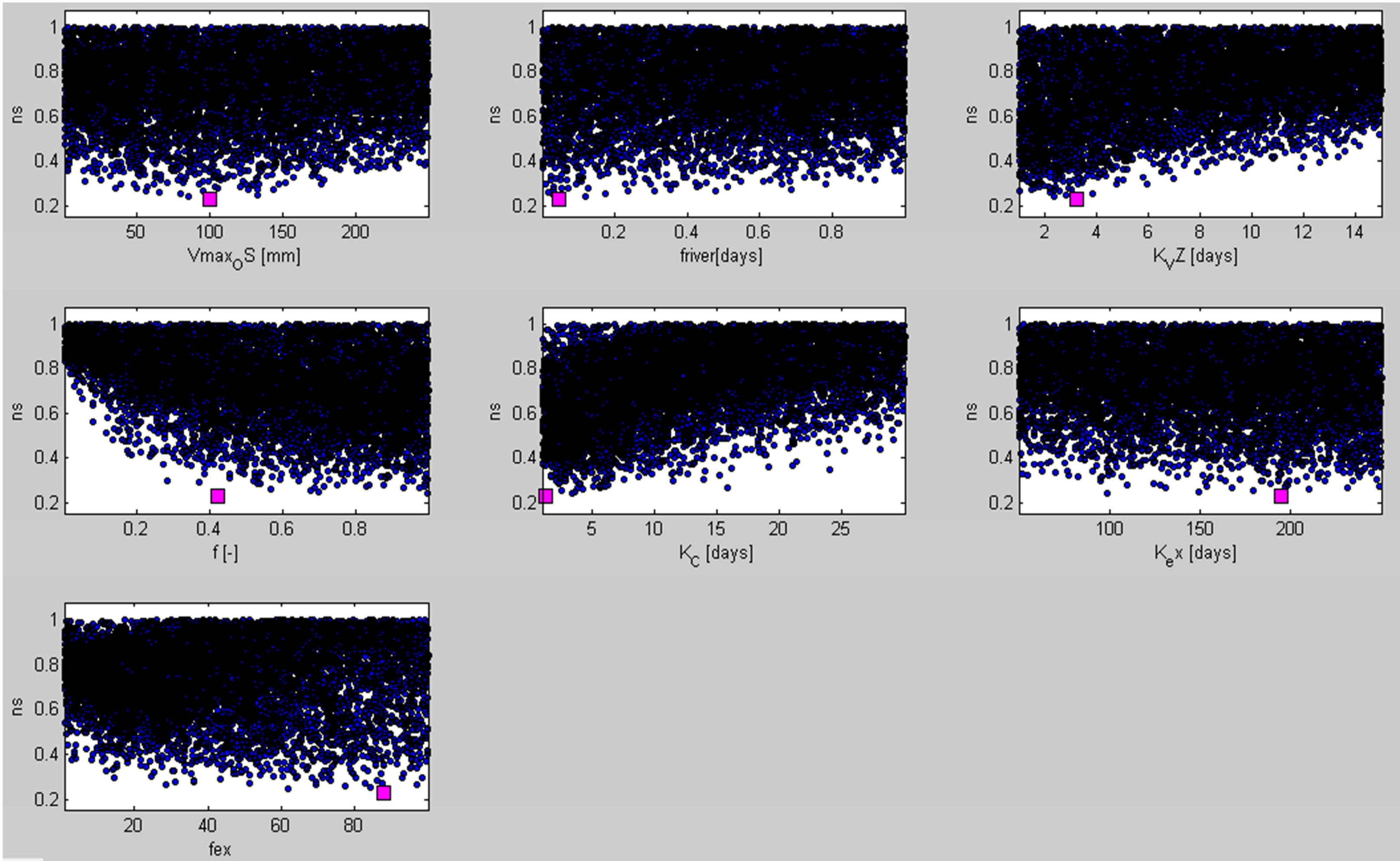

Fig 27 Exchange river-matrix model, 10000 iterations pear parameter and relative sensitivity functions.

d) Exchange river-conduits model

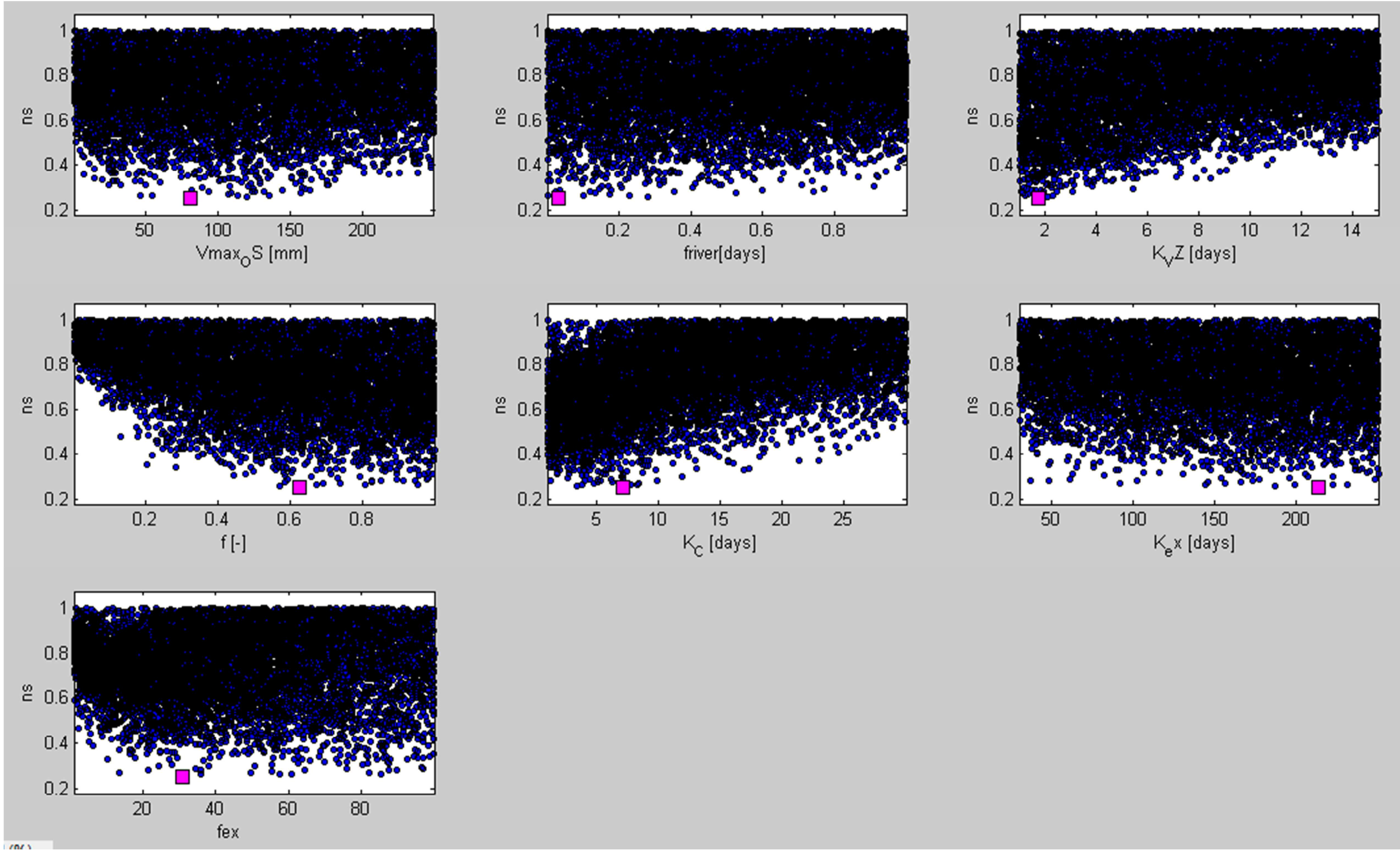

Fig 28 Exchange river-conduits model, 10000 iterations pear parameter and relative sensitivity functions.

8.3 RECHARGE RATE

In this part of the study, the recharge rate shows the realistic and unrealistic value of each parameter of the models. The realistic value is between 45-55%, and the other values are unrealistic. In the following graphs (Also in the Appendix A4) the values than less <45% were deleted.

In the figure 28 shows the range between 45-55% is realistic and majority of the points cloud are in this range, also the parameter value (K_C) are fit into the visual threshold between 0-8. Therefore the value is within the realistic range as a possible good fit value for this parameter. The points cloud is grouped in one place and it is not uniform. For all the models and methods this parameter has the same behavior.

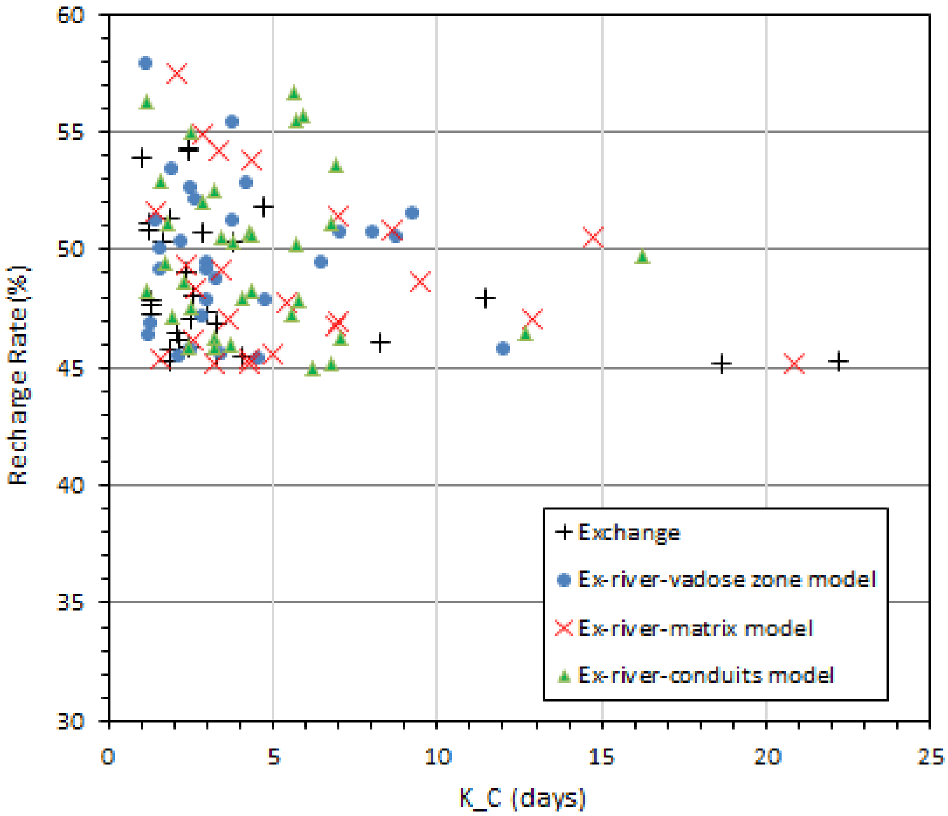

Fig 29 Parameter K_C vs. Recharge rate, for all models.

In the figure 29 the points cloud is uniform. The parameter friver has a very good recharge rate however the value is not important if is between 0 and 1. Hence the probability to have one value in all the parameter range is the same.

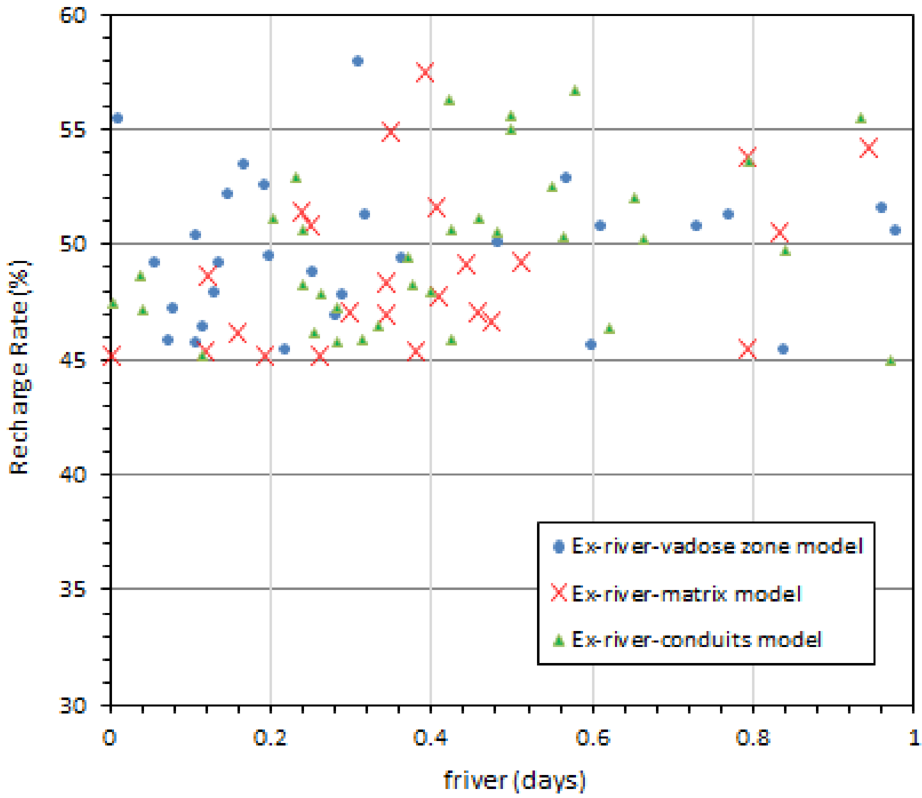

Fig 30 Parameter friver vs. Recharge rate, for all models.

In the appendix A4 shows all the Recharge rates graphics and it is evaluated all the parameters for each model.

9 DISCUSSION

It is analyzed the Shuffled Complex Evolution (SCE-UA) and Nash Sutcliffe efficiency (NSE) for all the models.

Calibration with SCE

The Exchange model shows (Figure 18) a good fit between the Auta discharge and the modelled data. In the table 2 all the parameters are set up with the realism of the data. Furthermore the parameter f is shown in more details. The f represents the input flow of the conduits that the result in the optimal set is unrealistic. The reason is because the value f is very close to 1 and it means that the all the flow is coming from the vadose zone just through the conduits and nothing for the matrix. Finally the coefficient NSE is good value in the efficiency of the model although this model not considers the river influence (Nash and Sutcliffe, 1970). Just in this model are used six parameters. The reason is to identify differences in all the models with river or not.

The Exchange river-vadose zone model shows (Figure 19) a good fit that it was described above. Since this model are used seven parameters. In the table 3 shows the extra parameter is the river influence that it is ''friver''. The parameter friver is very low, almost 0. It means, the friver have not been participated to recharge the aquifer. Furthermore the coefficient NSE is good but the parameters are not realistic.

The Exchange river-matrix and Exchange river-conduits models have the similar results explained above. In the table 4 and 5 the parameter friver still have the same value close to 0. In the table 6 shows the similar results by NSE in all the models. The efficiency is very good but the parameters considered in the models are unrealistic.

Monte Carlo sampling and Sensitivity analysis

The Monte Carlo sampling has a strong relationship with the sensitivity analysis, SCE-UA, and NSE. The Exchange model shows (Appendix 4, Figure 30) the parameters f, K_C, and K_VZ are sensitive. These three parameters have the most influence in the results of the models by them sensitivity. The Exchange river-vadose zone and the rest of the models are joined ''friver'' parameter and the three parameter sensitive remain sensitive without modification. (Appendix 4, Figure 31-33). In contrary, the friver and the rest of the other parameters are insensitive in all the models because of large number of parameters are not identifiable by just discharge. It confirms the less participation in the results of the models (Appendix 4).

The Monte Carlo sampling method shows the shape of the points cloud. The three parameters explained above (f, K_C, and K_VZ) don't have uniform shape of the points cloud because one range into of the visual threshold have the best fit to the model. At difference, the friver and the rest of the other parameters have a uniform shape of the points cloud. Whatever value for friver parameter doesn't have influence to the results of the model.

The recharge rate improves the understanding about the river influence. The friver parameter has uniform shape of points cloud (Figure 29) but it has a realistic recharge rate. The recharge rate is real because the percentage between output and input is mathematically correct (Chapter 8.3) but the river participated in the model by just small amount of the water (Close to 0). Therefore the high uncertainty of the recharge rate and the influence of the river under defined the model. It is necessary to implement extra information to improve the model as hydrochemical data. Hydrochemial information gives stability in the model and decreases the uncertainty.

The Exchange model was built with intentions to set up a base model and compare with the other models results that it was described above. The results of SCE-UA, NSE, Sensibility analysis, Monte Carlo sampling, and recharge rate were very close between them

One cause might be the models are considered a big amount of water in the recharge and not permit accept another recharge (Sabar River). This recharge is calculated with the recharge area that it may have been overestimated and considered area is not part of the recharge (Hartmann et al. 2013a).

Other cause might the influence of the river is insignificant to the aquifer Los Tajos-Sierra de Enmedio and probably the river flow are joined with the regional flow and recharge the aquifer beside called Tajos de Sabar.

Other cause could be the difficult quantification of the river influence (Beven, 2006; Perrin et al., 2001) only having the discharge data (output). Considering the recharge area and the river are inputs in the models. The recharge area has high level of uncertainty and the river is a variable to calculate.

The last cause might be that the models not represent the correct behavior of the aquifer, one option could be that the discharge of Auta spring was considered the sum of discharge of Auta spring and trop plein 1 Auta spring as a result the storage model of the vadose zone (linear reservoir storage) was simplified and not divided between matrix and conduits (Butscher and Huggenberger, 2008) as a result obtain separate discharge of the trop plein 1 Auta and the Auta spring.

10 CONCLUSION

The Auta spring has bee characterized in four models, Exchange model, Exchange river-vadose zone, Exchange river-matrix model, and Exchange river-conduits model. The difference between the first model and the others models is the parameter friver.

- The river storage doesn't have enough influence in every model (the value is close to 0). The reason could be not enough parameters in the models that it couldn't be similar to the reality and it does not reproduce the correct behavior of the aquifer as a result difficult to quantify the influence between the Sabar River and the aquifer.
- The uncertainty of the recharge area of the aquifer affects the process in the model. The recharge area is part of the mathematical process and has participation in all the storages including the river storage.
- The models were built and are obtained very good fit although the results not consider the Sabar River in the recharge of the aquifer.
- The methods of calibration and validation (SCE-UA, NSE, Sensibility analysis, Monte Carlo sampling, and recharge rate) were applying correctly in all the models obtained homogenous results.

For the future studies, it should be apply methods to evaluate the recharge rate for example, APLIS and others techniques for karst aquifers. It will help to minimize the uncertainty in one unknown parameter in the system.

The hydrochemical model is a good tool to understand and quantify the influence of the river in the aquifer, several open source software can help to find the answer. Or a model calibration should include hydrochemical information as Hartmann et al. (2013, 2014)

As with any model, this model depends mainly on the quality of data that is used to build it. Its potential can be developed further by implementing field work and data collection in Auta spring.

11 REFERENCES

Benjamin D. (2000). The hydrology and hydrogeology of heron island, the Great Barrier Reef: modelling natural recharge and tidal groundwater flow in a Coral Cay. Ph.D. thesis, Department of chemical engineering, University of Queensland, Australia.

Beven K. (2001). Rainfall-Runoff Modelling ''the primer''. Professor of Hydrology and Fluid dynamics, Lancaster University, United Kingdom.

Beven, K. J. (2006), A manifesto for the equifinality thesis, J. Hydrol., 320(1–2), 18–36.

Bunderlik J., Simonovic S. (2004). Calibration, verification, and sensitivity analysis of the HEC-HMS hydrologic model. CFCAS project: Assessment of water resources risk and vulnerability of changing climatic conditions. University of Western Ontario, Universoty of Waterloo, and Upper thames river conservation authority.

Butscher, C., and P. Huggenberger (2008), Intrinsic vulnerability assessment in karst areas: A numerical modeling approach, Water Resour. Res., 44, W03408, doi:10.1029/2007WR006277

Cocco M., Justi L., Alessandro F., Dos Santos L (2011). A hybrid shuffled complex evolution approach based on differential evolution for unconstrained optimization. Elsevier.

Chong-yu X. (2002). Textbook of hydrologic models (Lärobok i Avrinningsmodeller)- Uppsala University department of Earth sciences hydrology Sweden.

Christian J. (1996). Parameterization, calibration and validation of distributed hydrological models. Journal of Hydrology 198 (1997) 69-67.

Chow, V.T., Maidment, David R., and Mays, L.W. (1988). Applied Hydrology. McGRAW-HILL, New York.

Diaz-Ramirez J., Johnson B., McAnally W., Martin J. (2010). Comparison of lumped and distributed hydrologic models for the runoff simulation of a large watershed in Alabama and Mississippi. Northern gulf institute conference, http://www.northerngulfinstitute.org/outreach/conferences/2010/presentations/7-6_Diaz-Ramirez_06-MSU-03_Pres.pdf.

Ford, D. C., & Williams, P. W. (2007). Karst Hydrogeology and Geomorphology. Chichester: Wiley.

Hartmann, A., Barberá, J. A., Lange, J., Andreo, B., & Weiler, M. (2013). Progress in the hydrologic simulation of time variant recharge areas of karst systems – Exemplified at a karst spring in Southern Spain. Advances in Water Resources, 54, 149–160. doi:10.1016/j.advwatres.2013.01.010

Hartmann A., Mudarra M., M. Andreo, B., Marín, A., Wagener, T., & Lange, J. (2014). Modeling spatiotemporal impacts of hydroclimatic extremes on groundwater recharge at a Mediterranean karst aquifer. *Water Resources Research*, n/a–n/a. doi:10.1002/2014WR015685

Hoshin V., Kling H., Guillermo F. (2009). Decomposition of the mean squared error and NSE performance criteria: Implications for improving hydrological modelling.Elsevier

Krause P., Boyle D., Basel F. (2005). Comparison of different efficiency criteria for hydrological model. Comparison of different efficiency criteria for hydrological model. European geoscieces union – Advances in geosciences 5, 89–97.

Madsen H. (2000). Automatic calibration of a conceptual rainfall–runoff model using multiple objectives. Elsevier

Mudarra, 2012. Importancia de la zona no saturada y zona saturada en el funcionamiento hidrogeológico de los acuíferos carbonáticos. Caso de la Alta CAdena, Sierra de Enmedio y área de Los Tajos (Provincia de Málaga). Tesis Doctoral, Universidad de Málaga, 464 pp.

Mudarra M., B. Andreo B., Mudry J. (2012). Monitoring groundwater in the discharge area of a complex karst aquifer to assess the role of the saturated and unsaturated zones. Springer

Nash, J. E., and J. V. Sutcliffe (1970), River flow forecasting through conceptual models. Part I: A discussion of principles, J. Hydrol., 10, 282–290.

Perrin, C., C. Michel, and V. Andréassian (2001), Does a large number of parameters enhance model performance? Comparative assessment of common catchment model structures on 429 catchments, J. Hydrol., 241, 275–301

Rimmer A., Hartmann A. Simplified conceptual structures and analytical solutions for groundwater discharge using reservoir equations. Israel oceanographic and limnological research Ltd, Institute of hydrology, Freiburg University.

Saltelli, A., Ratto, M., Andres, T., Campolongo, F., Cariboni, J., Gatelli, D, Tarantola, S. (2008). Global sensitivity analysis: the primer. John Wiley & Sons.

Song X., Tang L., Lv X., Fang H., Gu H. (2012). Shuffled complex evolution approach for effective and efficient surface wave analysis. Elsevier

Wagener T., Wheater H. (2004). Monte-carlo analysis toolbox user manual, version 5. Department of Civil and Environmental Engineering, Penn State University, and Imperial College London, Unite States and Unite Kingdom.

Wangwongwiroj N., Schlutter F., Mark O. (2001). Application of an automatic calibration scheme for urban rainfall-runoff models in mouse. 4th DHI Software Conference, 6-8 June 2001. Springer.

APPENDIX A1

PARAMETERS TABLE

PARAMETERS	Units	Value	MODEL			
			Exchange model	Exchange-river-vadose zone model	Exchange-river-matrix model	Exchange-river-conduits model
INPUTS						
Precipitation	mm/day		X	X	X	X
Real Evapotranspiration	mm/day		X	X	X	X
River flow	m^3/sec			X	X	X
MODE PARAMETERS						
Vmax_OS	mm/day		X	X	X	X
init_OS	mm/day	0	X	X	X	X
init_VZ	mm/day	0	X	X	X	X
friver		between 0-1		X	X	X
K_VZ	day		X	X	X	X
f	-	between 0-1	X	X	X	X
init_M	mm/day	0	X	X	X	X
init_C	mm/day	0	X	X	X	X
K_C	day		X	X	X	X
K_E	day		X	X	X	X
f_{ex}	-	between 0-1	X	X	X	X

Table 7 Parameters of each model

APPENDIX A2

MODELS CODE

a) Exchange model

```
function [sim]=aExchangemodel(InFlow,Param)

global        method_name        observed_raw        observed_date_raw
observed_separator_raw criterion_index_raw input_date input_separator
modelled  modelled_date  modelled_date_raw  criterion_type  des_start
des_end

%Global Parameters
    Vmax_OS=Param(1);
    K_VZ=Param(2);
    f=Param(3);
    K_C=Param(4);
    K_ex=Param(5);
    fex=Param(6);
    init_OS=0; %initial condition of soil(dry period)
    init_C=0; % water stored in conduits zone after dry season [mm
    init_VZ=0; %initial condition of vadose zone(dry period)
    init_M=0;% %initial condition of matrix zone(dry period)
    A=8.98;  %Recharge Area in Km2
%Input separation
    Auprec=InFlow{1};
    Auetp=InFlow{2};

%model of soil
V_OS = zeros(1,(length(Auprec)));
V_OS(1) = init_OS;

Evap_a = zeros(1,(length(Auprec)));
Q_OS = zeros(1,(length(Auprec)));

for t = 2:length(Auprec)

    Evap_a(t)=Auetp(t)*V_OS(t-1)/Vmax_OS;
    V_OS(t) = V_OS(t-1) + (Auprec(t) - Evap_a(t));

    if V_OS(t)<0
        V_OS(t)=0;
        Q_OS(t) = 0;
    elseif V_OS(t) > Vmax_OS
        Q_OS(t) = V_OS(t)-Vmax_OS;
        V_OS(t) = Vmax_OS;
    elseif V_OS(t) <= Vmax_OS
        Q_OS(t) = 0;
    end
end




%model of vadose zone
in_VZ=Q_OS;

Q_VZ=zeros(size(in_VZ));
V_VZ=zeros(size(in_VZ));
```

```
for i=1:length(in_VZ)
    if i==1
        QoLS=init_VZ/K_VZ;
    else
        QoLS=V_VZ(i-1)/K_VZ;
    end
    Q_VZ(i)=in_VZ(i)+(QoLS-in_VZ(i))*exp(-1/K_VZ);
    V_VZ(i)=K_VZ*Q_VZ(i);
end
Q_VZ=Q_VZ';

% recharge separation
Q_in_C=f*Q_VZ;  %Q(mm/d)
Q_in_M=(1-f)*Q_VZ; %Q(mm/d)

in_M=Q_in_M;    %Matrix
V_M=zeros(size(in_M));

in_C=Q_in_C;   %Conduits
Q_Auta=zeros(size(in_C));
V_C=zeros(size(in_C));
Qex=zeros(size(in_C));

for i=1:length(in_M)
    if i==1
        Vo_M=init_M;
    else
        Vo_M=V_M(i-1);
    end

    if i==1
        Vo_C=init_C;
    else
        Vo_C=V_C(i-1);
    end

Voo_C=in_C(i)+((Vo_M-fex*Vo_C)/K_ex)-(Vo_C/K_C);
Voo_M=in_M(i)-((Vo_M-fex*Vo_C)/K_ex);

A1=-0.5*(1/K_C+(1+fex)/K_ex)+sqrt(0.25*(1/K_C+(1+fex)/K_ex)^2-
(1/(K_C*K_ex)));
A2=-0.5*(1/K_C+(1+fex)/K_ex)-sqrt(0.25*(1/K_C+(1+fex)/K_ex)^2-
(1/(K_C*K_ex)));
C1=K_C*(in_M(i)+in_C(i));
C2=(K_ex*in_M(i))+(K_C*fex)*(in_M(i)+in_C(i));
B1=((Voo_C-(A2*Vo_C)+(A2*C1))/(A1-A2));
B2=(Vo_C-B1-C1);
B3=((Voo_M-(A2*Vo_M)+(A2*C2))/(A1-A2));
B4=(Vo_M-B3-C2);

V_C(i)= B1*exp(A1)+B2*exp(A2)+C1;
V_M(i)= B3*exp(A1)+B4*exp(A2)+C2;

Qex(i)=(V_M(i)-(fex*V_C(i)))/K_ex;
Q_Auta(i)=V_C(i)/K_C;
```

```
end

% spring discharge of saturated zone [mm/day] the recharge area
% to be changed for [l/s]

Q_sim=((Q_Auta)*A*1e6)/(24*3600);

sim=Q_sim;
```

b) Exchange river-vadose zone model

```
function [sim]=bExrivervadosezone(InFlow,Param)

global      method_name      observed_raw      observed_date_raw
observed_separator_raw criterion_index_raw input_date input_separator
modelled  modelled_date  modelled_date_raw  criterion_type  des_start
des_end

%Global Parameters
    Vmax_OS=Param(1);
    friver=Param(2);
    K_VZ=Param(3);
    f=Param(4);
    K_C=Param(5);
    K_ex=Param(6);
    fex=Param(7);
    init_M=0;
    init_OS=0; %initial condition of soil(dry period)
    init_C=0; % water stored in conduits zone after dry season [mm]
    init_VZ=0; %initial condition of vadose zone(dry period)
    A=8.98;  %Recharge Area in Km2
%Input separation
    Auprec=InFlow{1};
    Auetp=InFlow{2};
    Auriver=InFlow{3};

%model

V_OS = zeros(1,(length(Auprec)));
V_OS(1) = init_OS;

Evap_a = zeros(1,(length(Auprec)));
Q_OS = zeros(1,(length(Auprec)));

for t = 2:length(Auprec)

    Evap_a(t)=Auetp(t)*V_OS(t-1)/Vmax_OS;
    V_OS(t) = V_OS(t-1) + (Auprec(t) - Evap_a(t));

    if V_OS(t)<0
        V_OS(t)=0;
        Q_OS(t) = 0;
    elseif V_OS(t) > Vmax_OS
        Q_OS(t) = V_OS(t)-Vmax_OS;
        V_OS(t) = Vmax_OS;
    elseif V_OS(t) <= Vmax_OS
        Q_OS(t) = 0;
    end
end




% river flow (m3/s) converted to mm/d
```

```
Q_river(t)=(Auriver(t)*1000*3600*24)*friver/(A*1e6);

in_VZ=Q_OS+Q_river(t);

%model of vadose zone
Q_VZ=zeros(size(in_VZ));
V_VZ=zeros(size(in_VZ));

for i=1:length(in_VZ)
    if i==1
        QoLS=init_VZ/K_VZ;
    else
        QoLS=V_VZ(i-1)/K_VZ;
    end
    Q_VZ(i)=in_VZ(i)+(QoLS-in_VZ(i))*exp(-1/K_VZ);
    V_VZ(i)=K_VZ*Q_VZ(i);
end
Q_VZ=Q_VZ';

% discharge separation
Q_in_C=f*Q_VZ; %Q(mm/d)
Q_in_M=((1-f)*Q_VZ);  %Q(mm/d)

in_M=Q_in_M;    %Matrix
V_M=zeros(size(in_M));

in_C=Q_in_C;   %Conduits
Q_Auta=zeros(size(in_C));
V_C=zeros(size(in_C));
Qex=zeros(size(in_C));

for i=1:length(in_M)
    if i==1
        Vo_M=init_M;
    else
        Vo_M=V_M(i-1);
    end

    if i==1
        Vo_C=init_C;
    else
        Vo_C=V_C(i-1);
    end

Voo_C=in_C(i)+((Vo_M-fex*Vo_C)/K_ex)-(Vo_C/K_C);
Voo_M=in_M(i)-((Vo_M-fex*Vo_C)/K_ex);

A1=-0.5*(1/K_C+(1+fex)/K_ex)+sqrt(0.25*(1/K_C+(1+fex)/K_ex)^2-
(1/(K_C*K_ex)));
A2=-0.5*(1/K_C+(1+fex)/K_ex)-sqrt(0.25*(1/K_C+(1+fex)/K_ex)^2-
(1/(K_C*K_ex)));
C1=K_C*(in_M(i)+in_C(i));
C2=(K_ex*in_M(i))+(K_C*fex)*(in_M(i)+in_C(i));
B1=((Voo_C-(A2*Vo_C)+(A2*C1))/(A1-A2));
B2=(Vo_C-B1-C1);
B3=((Voo_M-(A2*Vo_M)+(A2*C2))/(A1-A2));
B4=(Vo_M-B3-C2);
```

```
V_C(i)= B1*exp(A1)+B2*exp(A2)+C1;
V_M(i)= B3*exp(A1)+B4*exp(A2)+C2;

Qex(i)=(V_M(i)-(fex*V_C(i)))/K_ex;
Q_Auta(i)=V_C(i)/K_C;

end

% spring discharge of saturated zone [mm/d] time the recharge area
% to be changed for [l/s]

Q_sim=(Q_Auta)*A*1e6/(24*3600);

sim=Q_sim;
```

c) Exchange river-matrix model

```
function [sim]=cExrivermatrix(InFlow,Param)

global        method_name        observed_raw        observed_date_raw
observed_separator_raw criterion_index_raw input_date input_separator
modelled  modelled_date  modelled_date_raw  criterion_type  des_start
des_end

%Global Parameters
    Vmax_OS=Param(1);
    friver=Param(2);
    K_VZ=Param(3);
    f=Param(4);
    K_C=Param(5);
    K_ex=Param(6);
    fex=Param(7);
    init_M=0;
    init_OS=0; %initial condition of soil(dry period)
    init_C=0; % water stored in conduits zone after dry season [mm]
    init_VZ=0; %initial condition of vadose zone(dry period)
    A=8.98;  %Recharge Area in Km2
%Input separation
    Auprec=InFlow{1};
    Auetp=InFlow{2};
    Auriver=InFlow{3};

%model of soil
V_OS = zeros(1,(length(Auprec)));
V_OS(1) = init_OS;

Evap_a = zeros(1,(length(Auprec)));
Q_OS = zeros(1,(length(Auprec)));

for t = 2:length(Auprec)

    Evap_a(t)=Auetp(t)*V_OS(t-1)/Vmax_OS;
    V_OS(t) = V_OS(t-1) + (Auprec(t) - Evap_a(t));

    if V_OS(t)<0
        V_OS(t)=0;
        Q_OS(t) = 0;
    elseif V_OS(t) > Vmax_OS
        Q_OS(t) = V_OS(t)-Vmax_OS;
        V_OS(t) = Vmax_OS;
    elseif V_OS(t) <= Vmax_OS
        Q_OS(t) = 0;
    end
end



%model of vadose zone
```

```
in_VZ=Q_OS;

Q_VZ=zeros(size(in_VZ));
V_VZ=zeros(size(in_VZ));


for i=1:length(in_VZ)
    if i==1
        QoLS=init_VZ/K_VZ;
    else
        QoLS=V_VZ(i-1)/K_VZ;
    end
    Q_VZ(i)=in_VZ(i)+(QoLS-in_VZ(i))*exp(-1/K_VZ);
    V_VZ(i)=K_VZ*Q_VZ(i);
end
Q_VZ=Q_VZ';

% river flow (m3/s) converted to mm/d
Q_river(t)=(Auriver(t)*1000*3600*24)*friver/(A*1e6);

% discharge separation
Q_in_C=f*Q_VZ; %Q(mm/d)
Q_in_M=((1-f)*Q_VZ)+Q_river(t);  %Q(mm/d)

in_M=Q_in_M;    %Matrix
V_M=zeros(size(in_M));

in_C=Q_in_C;   %Conduits
Q_Auta=zeros(size(in_C));
V_C=zeros(size(in_C));
Qex=zeros(size(in_C));

for i=1:length(in_M)
    if i==1
        Vo_M=init_M;
    else
        Vo_M=V_M(i-1);
    end

    if i==1
        Vo_C=init_C;
    else
        Vo_C=V_C(i-1);
    end

Voo_C=in_C(i)+((Vo_M-fex*Vo_C)/K_ex)-(Vo_C/K_C);
Voo_M=in_M(i)-((Vo_M-fex*Vo_C)/K_ex);

A1=-0.5*(1/K_C+(1+fex)/K_ex)+sqrt(0.25*(1/K_C+(1+fex)/K_ex)^2-
(1/(K_C*K_ex)));
A2=-0.5*(1/K_C+(1+fex)/K_ex)-sqrt(0.25*(1/K_C+(1+fex)/K_ex)^2-
(1/(K_C*K_ex)));
C1=K_C*(in_M(i)+in_C(i));
C2=(K_ex*in_M(i))+(K_C*fex)*(in_M(i)+in_C(i));
B1=((Voo_C-(A2*Vo_C)+(A2*C1))/(A1-A2));
B2=(Vo_C-B1-C1);
```

```
B3=((Voo_M-(A2*Vo_M)+(A2*C2))/(A1-A2));
B4=(Vo_M-B3-C2);

V_C(i)= B1*exp(A1)+B2*exp(A2)+C1;
V_M(i)= B3*exp(A1)+B4*exp(A2)+C2;

Qex(i)=(V_M(i)-(fex*V_C(i)))/K_ex;
Q_Auta(i)=V_C(i)/K_C;

end

% spring discharge of saturated zone [mm/d] time the recharge area
% to be changed for [l/s]

Q_sim=(Q_Auta)*A*1e6/(24*3600);

sim=Q_sim;
```

d) Exchange river-conduits model

```
function [sim]=dExriverconduits(InFlow,Param)

global    method_name    observed_raw    observed_date_raw
observed_separator_raw criterion_index_raw input_date input_separator
modelled  modelled_date  modelled_date_raw  criterion_type  des_start
des_end

%Global Parameters
   Vmax_OS=Param(1);
    friver=Param(2);
    K_VZ=Param(3);
    f=Param(4);
    K_C=Param(5);
    K_ex=Param(6);
    fex=Param(7);
    init_M=0;
    init_OS=0; %initial condition of soil(dry period)
    init_C=0; % water stored in conduits zone after dry season [mm]
    init_VZ=0; %initial condition of vadose zone(dry period)
    A=8.98;  %Recharge Area in Km2
%Input separation
    Auprec=InFlow{1};
    Auetp=InFlow{2};
    Auriver=InFlow{3};

%model

V_OS = zeros(1,(length(Auprec)));
V_OS(1) = init_OS;

Evap_a = zeros(1,(length(Auprec)));
Q_OS = zeros(1,(length(Auprec)));

for t = 2:length(Auprec)

    Evap_a(t)=Auetp(t)*V_OS(t-1)/Vmax_OS;
    V_OS(t) = V_OS(t-1) + (Auprec(t) - Evap_a(t));

    if V_OS(t)<0
        V_OS(t)=0;
        Q_OS(t) = 0;
    elseif V_OS(t) > Vmax_OS
        Q_OS(t) = V_OS(t)-Vmax_OS;
        V_OS(t) = Vmax_OS;
    elseif V_OS(t) <= Vmax_OS
        Q_OS(t) = 0;
    end
end
Q_OS=Q_OS';

%model of vadose zone
in_VZ=Q_OS;
```

```
Q_VZ=zeros(size(in_VZ));
V_VZ=zeros(size(in_VZ));

for i=1:length(in_VZ)
    if i==1
        QoLS=init_VZ/K_VZ;
    else
        QoLS=V_VZ(i-1)/K_VZ;
    end
    Q_VZ(i)=in_VZ(i)+(QoLS-in_VZ(i))*exp(-1/K_VZ);
    V_VZ(i)=K_VZ*Q_VZ(i);
end

% river flow (m3/s) converted to mm/d
Q_river(t)=(Auriver(t)*1000*3600*24)*friver/(A*1e6);

% discharge separation
Q_in_C=f*Q_VZ + Q_river(t); %Q(mm/d)
Q_in_M=((1-f)*Q_VZ);  %Q(mm/d)

in_M=Q_in_M;    %Matrix
V_M=zeros(size(in_M));

in_C=Q_in_C;   %Conduits
Q_Auta=zeros(size(in_C));
V_C=zeros(size(in_C));
Qex=zeros(size(in_C));

for i=1:length(in_M)
    if i==1
        Vo_M=init_M;
    else
        Vo_M=V_M(i-1);
    end

    if i==1
        Vo_C=init_C;
    else
        Vo_C=V_C(i-1);
    end

Voo_C=in_C(i)+((Vo_M-fex*Vo_C)/K_ex)-(Vo_C/K_C);
Voo_M=in_M(i)-((Vo_M-fex*Vo_C)/K_ex);

A1=-0.5*(1/K_C+(1+fex)/K_ex)+sqrt(0.25*(1/K_C+(1+fex)/K_ex)^2-
(1/(K_C*K_ex)));
A2=-0.5*(1/K_C+(1+fex)/K_ex)-sqrt(0.25*(1/K_C+(1+fex)/K_ex)^2-
(1/(K_C*K_ex)));
C1=K_C*(in_M(i)+in_C(i));
C2=(K_ex*in_M(i))+(K_C*fex)*(in_M(i)+in_C(i));
B1=((Voo_C-(A2*Vo_C)+(A2*C1))/(A1-A2));
B2=(Vo_C-B1-C1);
B3=((Voo_M-(A2*Vo_M)+(A2*C2))/(A1-A2));
B4=(Vo_M-B3-C2);
```

```
V_C(i)= B1*exp(A1)+B2*exp(A2)+C1;
V_M(i)= B3*exp(A1)+B4*exp(A2)+C2;

Qex(i)=(V_M(i)-(fex*V_C(i)))/K_ex;
Q_Auta(i)=V_C(i)/K_C;

end

% spring discharge of saturated zone [mm/d] time the recharge area
% to be changed for [l/s]

Q_sim=(Q_Auta)*A*1e6/(24*3600);

sim=Q_sim;
```

APPENDIX A3

SENSITIVITY ANALYSIS

a. Exchange model

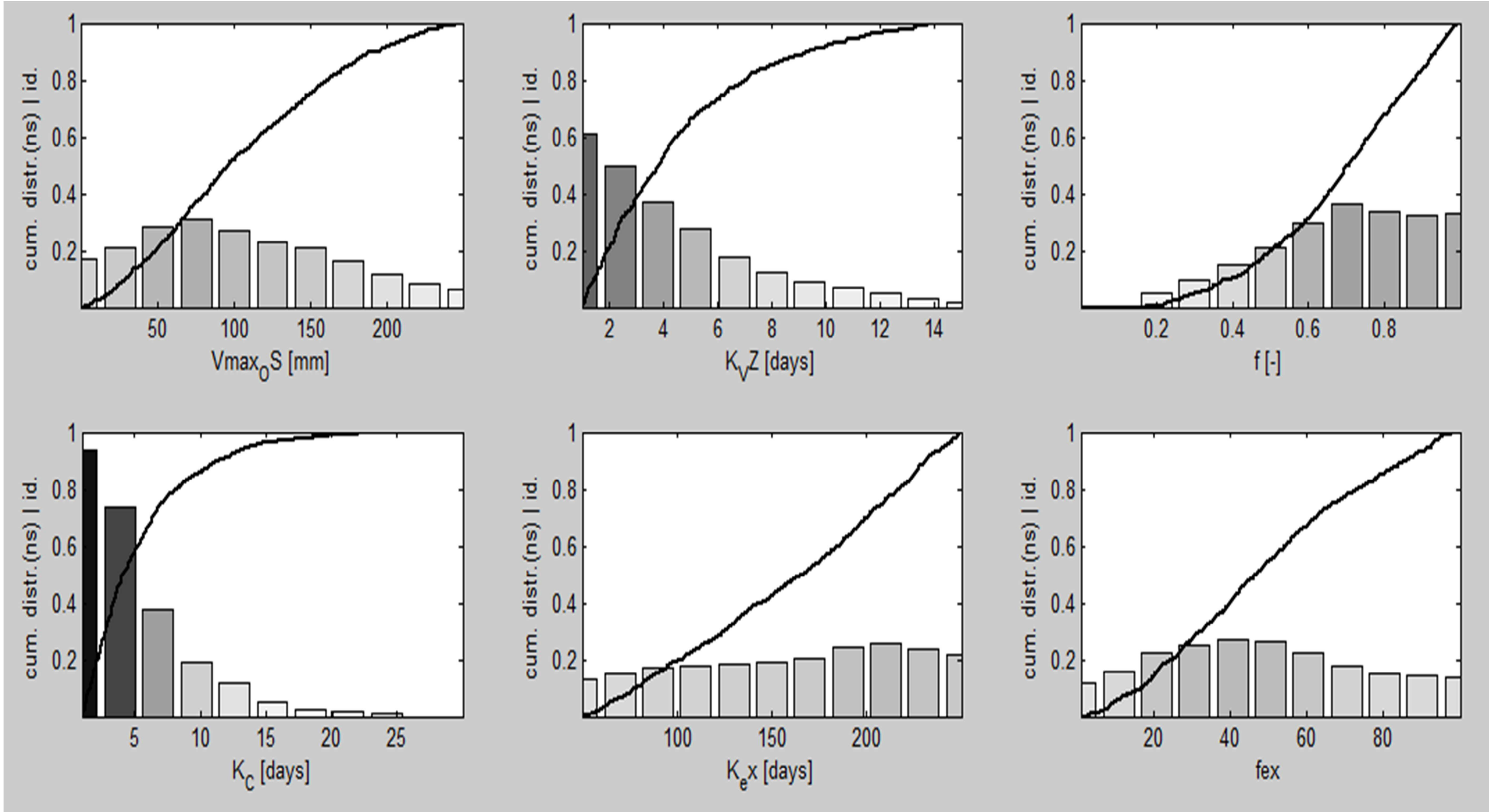

Fig 31 Exchange model, parameters frequency and relative sensitivity functions.

b. Exchange river-vadose zone model

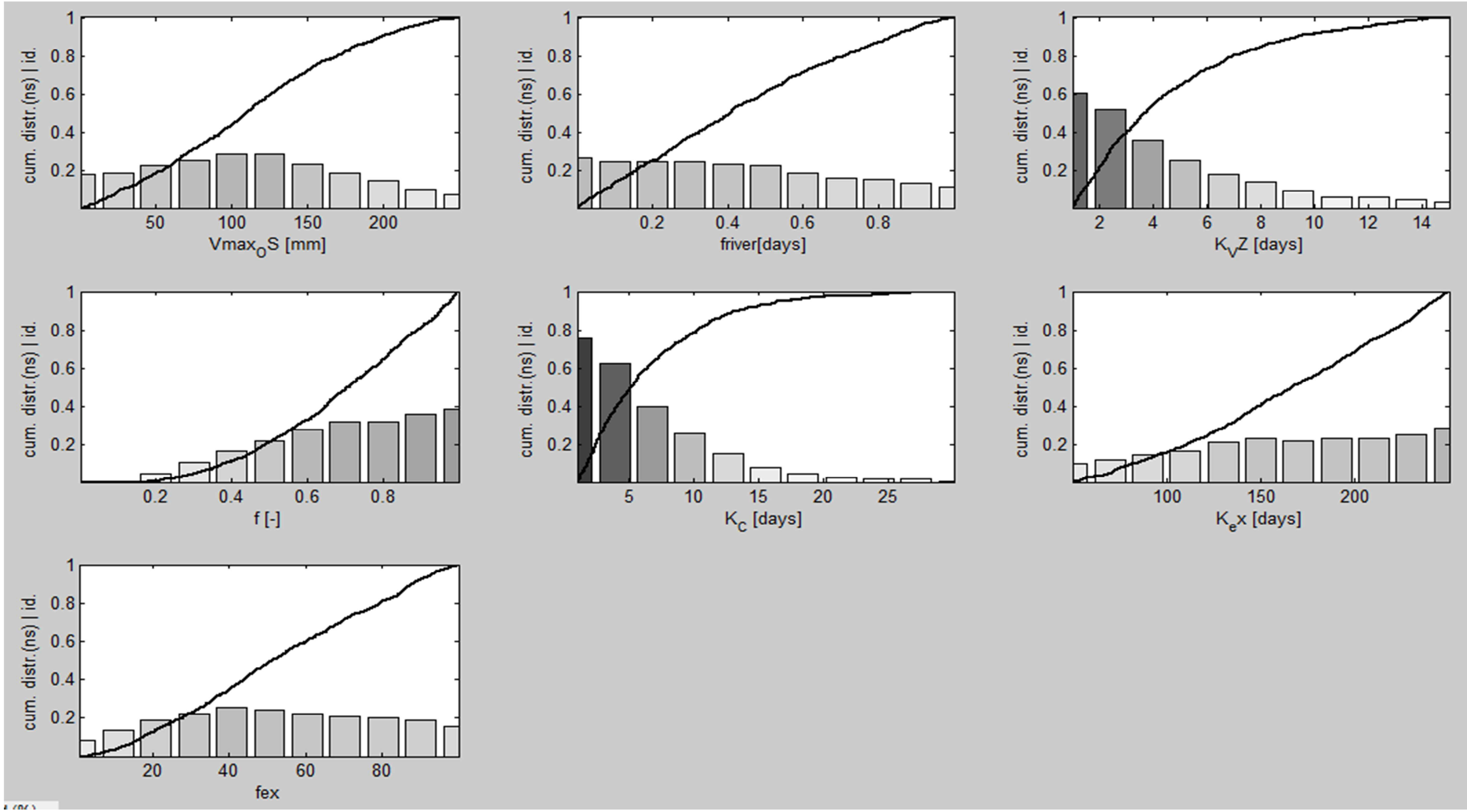

Fig 32 Exchange river-vadose zone model, parameters frequency and relative sensitivity functions.

c. Exchange river-matrix model

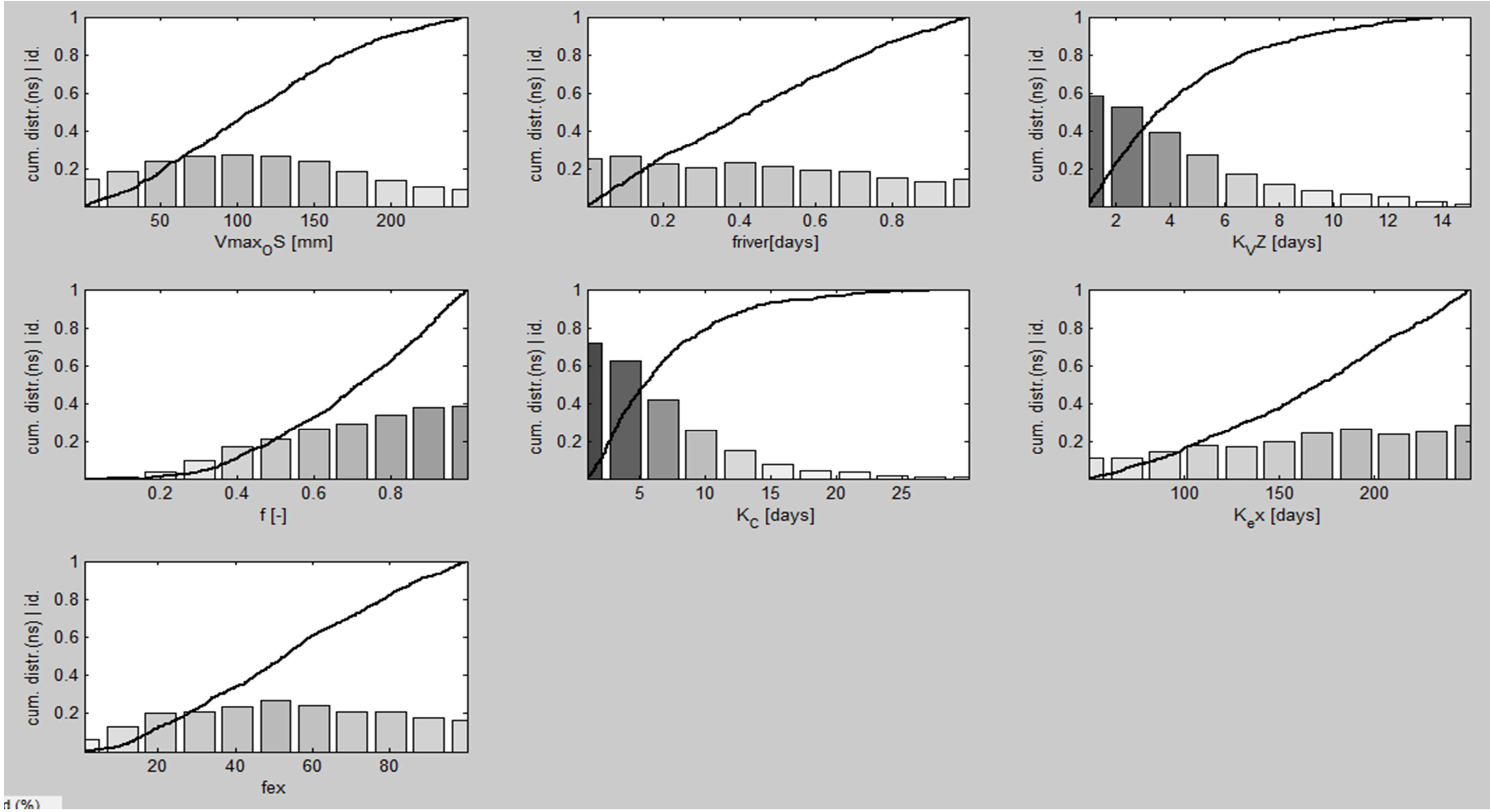

Fig 33 Exchange river-matrix model, parameters frequency and relative sensitivity functions.

d. <u>Exchange river-conduits model</u>

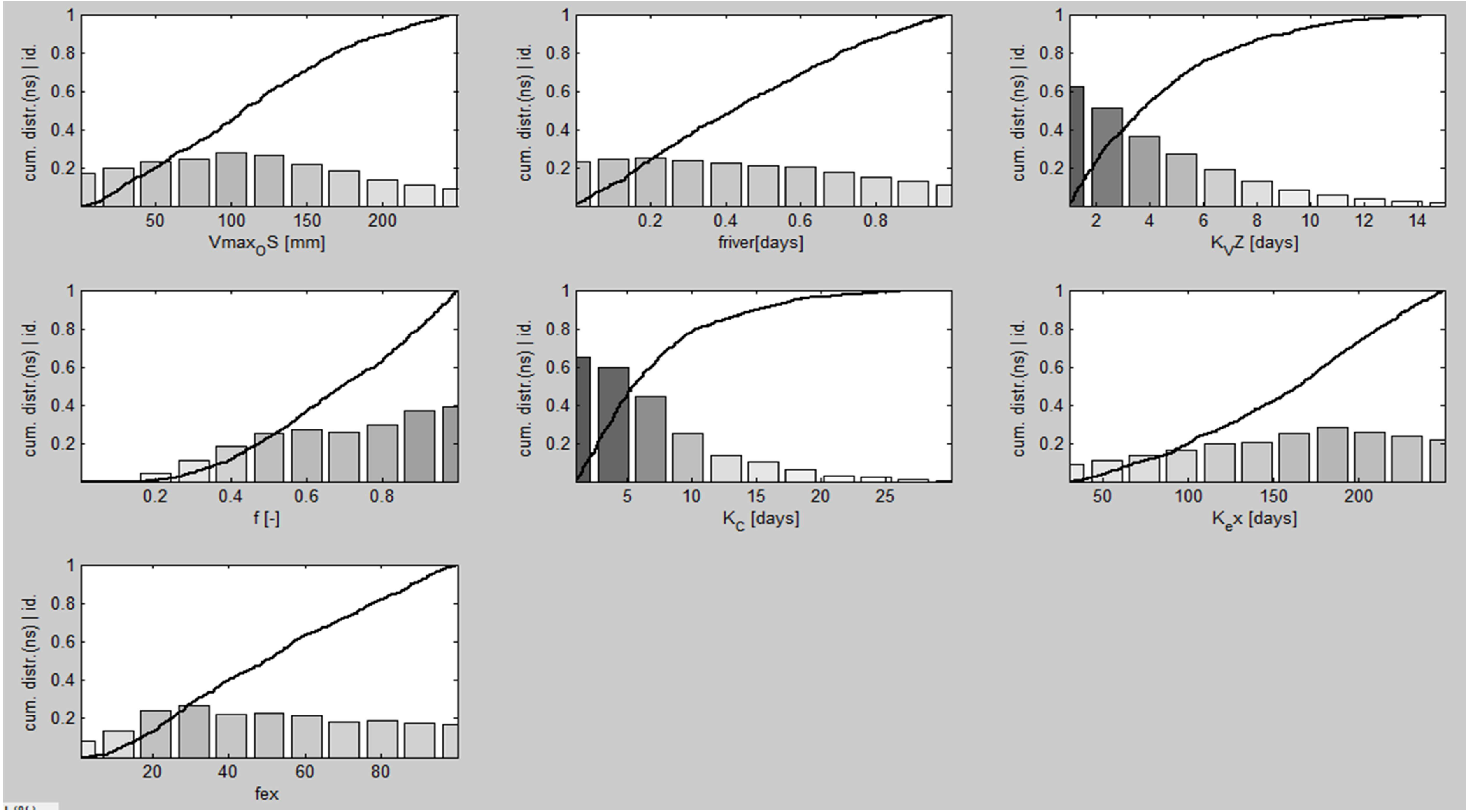

Fig 34 Exchange river-conduits model, parameters frequency and relative sensitivity functions.

APPENDIX A4

TABLES OF RECHARGE RATE AND GRAPHICS

a. Exchange model

Rechargue Rate	NSE = 1- NS	Vmax_OS [mm]	K_VZ [days]	f [-]	K_C [days]	K_ex [days]	fex
54.33169749	0.683632457	62.09134711	1.111922225	0.278991904	2.424734723	64.26510236	9.927561432
54.20726113	0.686794077	26.98381325	3.504589192	0.746551427	2.434587153	64.25697639	49.42342644
53.96176963	0.679331359	48.0792084	4.358824587	0.770641849	1.028835174	59.95295061	81.78330464
51.87109165	0.655169774	10.82603939	3.149889796	0.718313564	4.730661671	94.15778473	45.90238471
51.30091477	0.692075059	32.66289934	1.718980258	0.627506477	1.843539004	77.23892193	69.76100427
51.10860599	0.713868846	42.0731734	2.96645572	0.532449752	1.206638005	64.35329779	85.35089299
50.86019225	0.663231224	79.31896894	5.618791966	0.411162656	1.204762379	94.18708305	19.46225547
50.6894974	0.674509503	22.56766992	1.241399326	0.231177463	2.860212557	150.8210912	24.14454728
50.3464938	0.650627349	51.03481076	3.582066511	0.859332964	1.668161907	96.00066519	78.04489546
50.30902088	0.716636298	38.75165206	2.138208128	0.628262216	3.811745552	56.6865448	33.03739471
49.00715465	0.66843504	11.91856659	3.987328738	0.475938991	2.391658567	189.3482383	80.52980849
48.09386788	0.651781415	50.09816007	1.577634064	0.556677578	2.583650028	136.1534056	42.96292458
47.96442792	0.658438083	1.379099266	1.198993496	0.9731447	11.44657251	138.8724506	43.71454201
47.89706086	0.725800677	84.5244297	5.115622742	0.746313428	1.299761932	59.68946785	67.12369604
47.64571977	0.67826724	28.6671083	1.173739244	0.216227329	1.331398336	178.4898531	52.18210301
47.39657507	0.696982579	23.70827756	1.884036073	0.816480683	2.984997201	109.5270459	78.96950028
47.31167987	0.667969197	109.1644999	5.65803566	0.485961304	1.318460234	60.77164863	36.37204477
47.07605241	0.742584815	56.38957785	2.875647464	0.536674924	2.517170204	101.144681	45.12894573
46.86216607	0.691876813	39.28739365	2.117015114	0.27566186	3.291082409	193.3633217	17.51183483
46.50628603	0.700207511	104.1914254	4.924100133	0.598100317	2.057770844	62.73730061	32.96536801
46.18133567	0.694668077	24.5946326	3.380624768	0.371163799	2.153087056	191.8481907	64.49279466
46.04192987	0.710920591	50.26133542	1.600079706	0.639163201	8.301000028	133.97679	18.01178764
45.84555418	0.670812206	114.3359367	3.336580996	0.344455816	2.461455149	68.71724723	17.20440036
45.80327195	0.654898589	45.57673941	8.831489803	0.626474489	1.873769921	178.4546115	83.97795204
45.61449787	0.676632336	36.64002433	4.678840577	0.649761061	3.285418974	212.2034267	58.95975201
45.4882786	0.749614172	86.95531174	1.775439704	0.819441443	4.075169808	51.21480931	28.2291929
45.26276154	0.659216902	83.4617708	3.874434904	0.494357068	1.90505983	215.514883	27.16148634
45.24548039	0.654049376	22.27741213	1.061921026	0.934334249	22.21436511	214.2372576	14.98654206
45.21152626	0.671265552	50.84497884	1.160061963	0.854607436	18.64312725	56.75961305	9.082106636

Table 8 Recharge rate, Nash Sutcliffe efficiency and parameters set, exchange model.

b. Exchange river-vadose zone model

Rechargue Rate	NSE = 1- NS	Vmax_OS [mm]	friver[days]	K_VZ [days]	f [-]	K_C [days]	K_ex [days]	fex
58.03034821	0.650194263	67.48645093	0.307820759	4.843260736	0.59143067	1.12741261	76.2838927	82.5256113
55.48614418	0.675416804	19.50157269	0.010257214	1.441079408	0.60532263	3.6986129	50.0166118	33.1093192
53.53923573	0.702938468	51.95500969	0.164448372	3.040430157	0.63094766	1.84733161	84.5754049	65.6029025
52.92552451	0.68381405	62.26488966	0.566049692	3.282608904	0.95112328	4.14217847	104.963767	74.3935662
52.67474599	0.656863618	36.95598302	0.192020239	3.300617902	0.79511184	2.42754719	135.425393	82.3591228
52.25823738	0.693384417	75.83184318	0.145703146	2.894131241	0.41157062	2.56652729	100.52963	22.5108594
51.65714672	0.663429601	69.86343492	0.959018524	1.804934676	0.72463417	9.20213997	244.505442	51.6332795
51.34636873	0.665725353	75.94091571	0.767730341	3.80868241	0.61220866	3.74867727	222.179305	89.4488088
51.30879203	0.657278167	139.0980599	0.316260137	6.137286211	0.68654635	1.35247075	108.247546	73.0795755
50.82979301	0.657922039	24.87765312	0.611155295	1.198022584	0.88110747	6.99040024	243.95351	74.8006423
50.82121155	0.681842887	77.20306595	0.728478495	1.246489901	0.62266376	7.99187105	154.953016	40.3910017
50.64266371	0.694317934	102.0007845	0.974842473	1.715198146	0.9419527	8.71923824	189.107276	58.4286861
50.45522295	0.666161955	60.23241116	0.106333094	1.60606097	0.44678869	2.15462862	144.60765	36.6245988
50.16132413	0.652665936	176.2149639	0.482273851	4.183489723	0.69044581	1.51923952	94.6310408	91.468646
49.57052027	0.661204618	13.37228314	0.195737101	2.969675311	0.88679416	6.44464587	131.801757	55.0260391
49.5237709	0.713418953	80.67661325	0.360732	2.078072432	0.66114131	2.91835156	84.3813914	67.9268043
49.29412788	0.714821266	57.51161276	0.055536518	1.394096107	0.25185329	2.95239082	134.112311	14.745953
49.29367107	0.687554003	79.0368596	0.135414804	5.79465898	0.61847513	1.52708279	163.068977	67.2400008
48.882489	0.717558063	76.35441315	0.251421439	2.74273419	0.64567496	3.2071636	77.6530354	52.3989967
47.93875885	0.732621502	60.50190584	0.129343097	1.754518026	0.38083215	2.9541672	138.163627	35.8563602
47.91723054	0.681496861	28.03779959	0.286626162	1.390523084	0.99149492	4.6841644	111.625358	78.6935261
47.27699143	0.744973094	73.33883416	0.079786702	2.071790244	0.42539255	2.79048239	109.848036	33.0057889
46.99252207	0.696734463	127.9442766	0.279567689	6.111713806	0.52655923	1.21538184	203.174673	84.4245833
46.49241363	0.684342757	122.042475	0.113914387	4.863526544	0.45825353	1.19549368	75.512641	61.796856
45.88644944	0.672598233	12.20248344	0.070519226	1.57780309	0.83239762	11.9344645	139.664739	30.4226411
45.8303601	0.704226498	33.22868848	0.106569198	3.387186543	0.46092947	2.47348902	183.983895	78.0234791
45.64787702	0.659271672	175.7739412	0.59732101	1.587807327	0.97236216	3.3349634	122.721447	93.0542002
45.56226381	0.682500004	73.96103427	0.218551911	1.46828386	0.44371662	2.11489463	242.969029	64.0704938
45.49631527	0.652142946	170.2728503	0.836511745	1.944747182	0.52945037	4.51173203	220.187716	72.1692568

Table 9 Recharge rate, Nash Sutcliffe efficiency and parameters set, Exchange river-vadose zone model.

c. Exchange river-matrix model

Rechargue Rate	NSE = 1- NS	max_OS [mm	friver[days]	K_VZ [days]	f [-]	K_C [days]	K_ex [days]	fex
57.4621604	0.655530579	45.4836221	0.39404268	1.23120762	0.29515086	2.10629338	144.841276	40.3711177
54.9254015	0.652837944	36.2446768	0.35001977	1.9510283	0.94000881	2.83826294	81.3408555	79.6478491
54.17987972	0.656272971	88.8308381	0.94532872	2.38332878	0.55593896	3.38037478	223.113387	75.2278332
53.80535895	0.660409126	88.450389	0.79442699	1.69679112	0.77098642	4.33313243	135.035818	63.5205264
51.59612457	0.695938404	109.640404	0.40620119	3.05764265	0.38791011	1.4168891	184.023255	46.2221825
51.41425303	0.709815887	76.7105068	0.24122105	1.19360723	0.55189314	7.01601707	91.450574	15.9182244
50.82539631	0.651686961	41.6625482	0.25108861	1.69870554	0.54390346	8.59513868	164.077118	19.1928526
50.50625876	0.651903033	49.6359724	0.83363978	1.51449675	0.96455149	14.7715615	159.273397	29.9627485
49.30066203	0.692941056	126.512611	0.51376506	3.21106842	0.46451432	2.40504	180.282186	55.4221376
49.16309553	0.699393028	104.707692	0.44372229	3.32150436	0.82195928	3.43864555	126.499795	61.8842183
48.68700724	0.673699862	48.9066089	0.12218834	2.83922008	0.98811843	9.49938066	51.6113352	19.8514128
48.36457309	0.666955599	113.666539	0.34433239	4.29415502	0.43010915	2.67792651	156.131611	37.5279637
47.79800815	0.707589315	126.408924	0.41155443	1.24080428	0.42770758	5.40197197	178.234528	20.129135
47.11308813	0.667121944	88.3224885	0.45772645	1.20445103	0.65247021	12.8900712	111.515824	18.0569018
47.06002139	0.693261828	43.0040843	0.29860659	3.8520407	0.72727613	3.642077	137.258189	77.7398134
46.984176	0.662126016	60.5410883	0.34622379	2.47483005	0.84140879	6.99310391	208.219086	42.711336
46.73672612	0.714564343	127.128804	0.47533513	1.5044206	0.82548226	6.95686929	116.704906	33.5179952
46.206599	0.741924816	78.6373401	0.15853315	3.53521404	0.64597678	2.55767965	105.393749	61.7813182
45.52707081	0.686436907	141.530015	0.7928686	2.06940409	0.75157445	4.99694678	245.405312	68.6313547
45.42519525	0.699722452	137.768428	0.12088326	1.50805045	0.62267121	1.61111152	55.6592199	58.9532609
45.39309694	0.661135943	98.8020712	0.38206601	1.28406947	0.88258929	4.28500704	133.165866	62.702852
45.18134107	0.722636231	95.6359292	0.00382708	4.65322289	0.8362249	3.21417686	64.5577799	34.6560369
45.169666	0.652906668	98.2465706	0.19414242	1.14535071	0.83202961	20.8683751	77.6368085	7.86681734
45.1680205	0.728907322	50.3656625	0.26226973	2.65545696	0.93664339	4.3277779	130.306512	75.4132295

Table 10 Recharge rate, Nash Sutcliffe efficiency and parameters set, Exchange river-matrix model.

d. Exchange river-conduits model

Rechargue Rate	NSE = 1- NS	max_OS [mm	friver[days]	K_VZ [days]	f [-]	K_C [days]	K_ex [days]	fex
56.70087731	0.653812264	65.1472141	0.5764011	1.50231696	0.99605605	5.6238707	73.25326134	43.4747579
56.28736134	0.66546745	100.341636	0.42038156	2.14281437	0.48608258	1.17224158	112.3174286	83.9650223
55.6615976	0.674892851	82.8063604	0.49738006	2.2345061	0.90606018	5.94592553	53.84891613	31.2813022
55.48664563	0.651941047	114.396132	0.93424774	2.22019599	0.64953289	5.72284009	176.928012	56.8920257
55.00180711	0.677921602	68.740415	0.49632705	3.40964795	0.66413782	2.5134138	109.1881616	81.7089034
53.63817879	0.665269167	82.9050822	0.79562016	1.92379705	0.85009865	6.94361249	196.23879	55.72607
52.9233334	0.654144303	60.2343933	0.23007328	6.20572905	0.73442471	1.6067329	178.1628677	98.8963957
52.53810834	0.671648951	102.992817	0.54938185	3.43582667	0.60159903	3.22746892	225.0613077	65.4600938
52.02636337	0.699022027	111.6699	0.65213536	3.18455673	0.8800416	2.88067822	102.6259391	97.1723865
51.15840307	0.657586469	103.722633	0.20244423	3.5473163	0.58081689	1.78548195	127.8898644	45.2326255
51.11926228	0.677713913	141.836175	0.45629019	1.92101564	0.77708731	6.77915363	93.68142814	24.3882752
50.69248646	0.683148324	132.381401	0.42408585	2.89053752	0.6781008	4.2599329	78.44924848	36.5972908
50.67456015	0.650204605	43.8677237	0.24111046	4.46926179	0.68399919	4.39128089	144.699293	48.5131005
50.49295995	0.670950351	88.4478102	0.47944716	4.32474633	0.70602418	3.47466428	239.129991	75.4618439
50.30733136	0.664790466	89.512996	0.56470611	5.35832368	0.85653873	3.77562059	230.5571291	92.1218724
50.22051849	0.675569452	56.3629314	0.66294404	3.44971147	0.89932514	5.69609664	178.4233358	78.1778084
49.71314055	0.654668011	68.9532049	0.83920026	1.15756905	0.97909006	16.2355627	110.7212839	28.561556
49.46169934	0.668848727	136.82569	0.37163585	6.71717766	0.85031221	1.73501033	109.665494	99.5877522
48.69601785	0.705393158	73.9001386	0.03993929	5.88592614	0.95316152	2.307699	72.07348564	54.7894243
48.25377763	0.653966139	75.996161	0.37558873	3.12460678	0.38762515	4.37248583	230.0459698	38.1425282
48.22428799	0.690442632	101.999516	0.24010786	3.08958654	0.28240554	1.13732815	131.2780853	69.5318192
47.99044388	0.660420605	118.960332	0.39896596	4.46551819	0.61208331	4.07530151	172.5824576	47.0463424
47.90170432	0.680346911	66.2532996	0.26169523	2.74015544	0.56100471	5.81692569	191.0670714	32.8197487
47.51901828	0.736603471	91.531816	0.00263269	3.5165247	0.93904849	2.53615296	41.17038272	37.3032753
47.28294139	0.709501655	44.5883149	0.28288604	2.18808774	0.69404491	5.56167592	163.8862322	52.5928857
47.17271933	0.652165049	59.9758177	0.04098587	4.55038133	0.25186274	1.91999583	189.624021	12.7867207
46.50254838	0.657512324	84.1289427	0.33359317	2.07001247	0.75235054	12.6536554	193.0260154	20.7294049
46.30678341	0.658265926	79.6396357	0.61990054	4.93666876	0.99992236	7.04170176	203.6215649	70.9868075
46.22299437	0.73245655	75.126451	0.25361316	2.16547805	0.52556434	3.23471447	205.7887716	58.4979014
45.92418579	0.682364623	41.2113172	0.42417506	2.05548271	0.4575088	3.70844995	224.2068279	91.3415649
45.90291846	0.669635223	122.223264	0.31397254	3.55788426	0.51301375	3.25593433	101.8881052	50.5568345
45.83235135	0.729972048	116.984643	0.28252569	3.31491387	0.49815027	2.43587608	167.8701356	60.8897859
45.18188193	0.686544697	83.3581661	0.11408826	2.56623407	0.73456986	6.79448251	156.2570555	25.450562
45.01312766	0.673605737	113.473699	0.96864215	2.02076388	0.90415512	6.19910085	137.7103614	93.3768226

Table 11 Recharge rate, Nash Sutcliffe efficiency and parameters set, Exchange river-conduits model.

Parameter friver

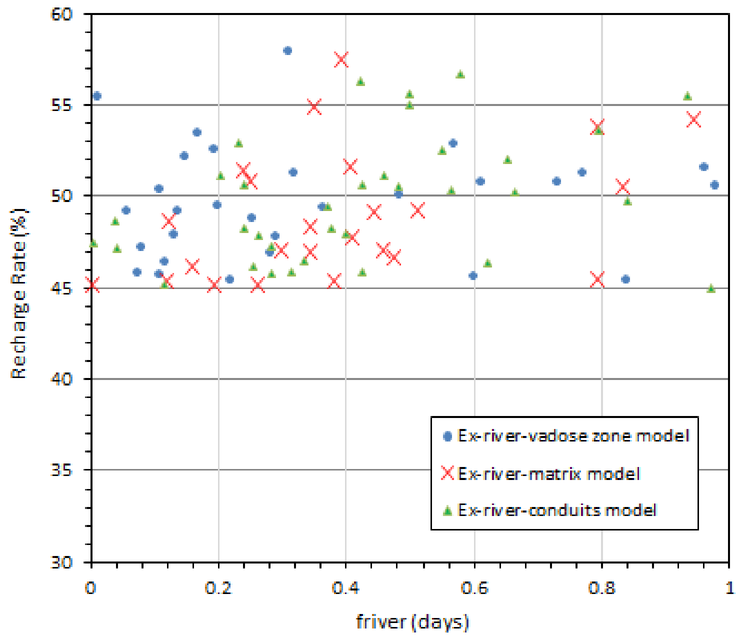

Fig 35 Recharge rate vs. friver for all models.

Parameter K_VZ

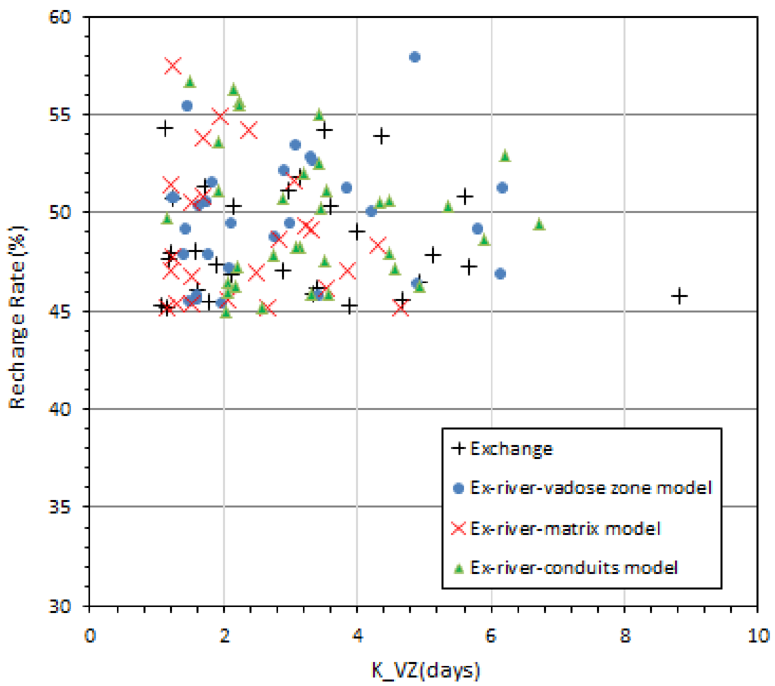

Fig 36 Recharge rate vs. K_VZ for all models.

Parameter K_C

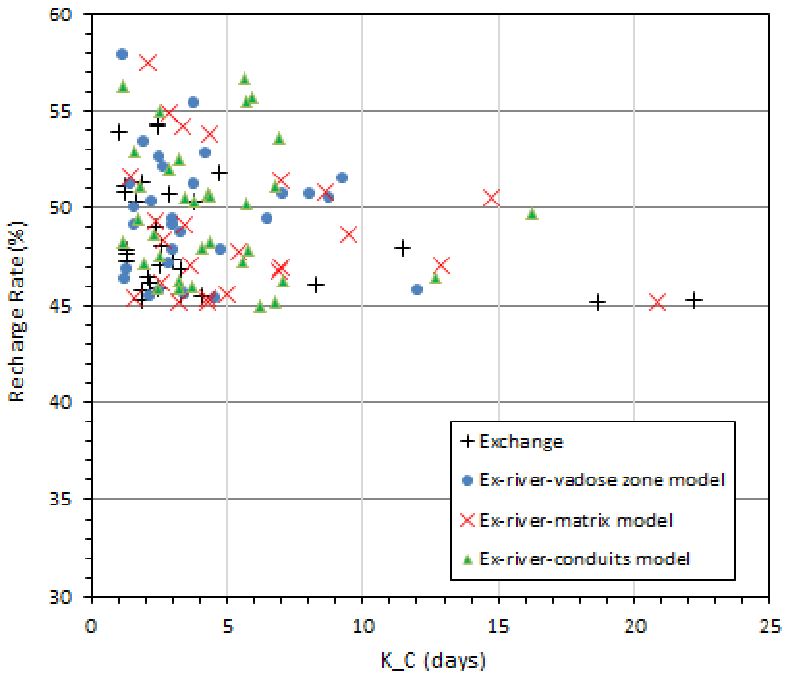

Fig 37 Recharge rate vs. K_C for all models.

Parameter K_E

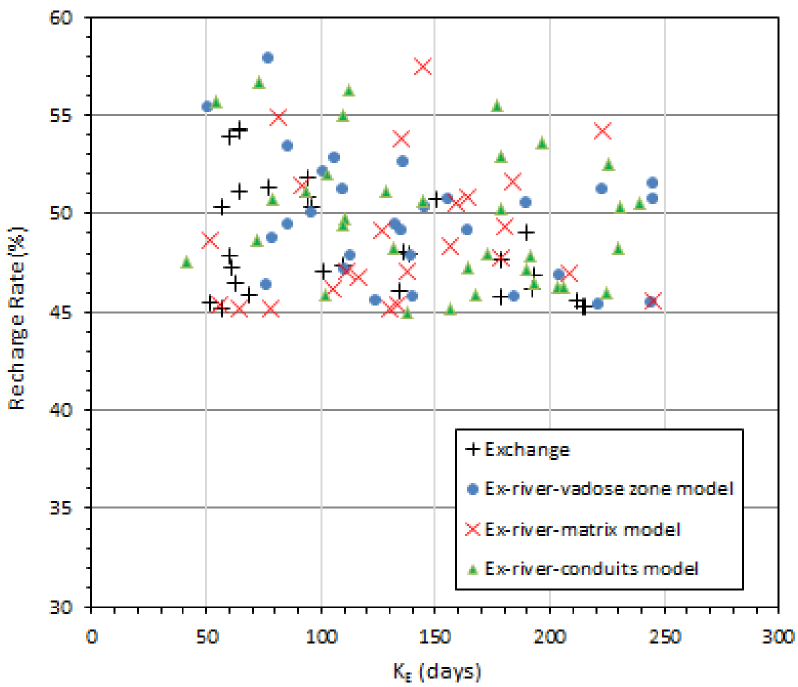

Fig 38 Recharge rate vs. KE for all models.

Parameter f_{ex}

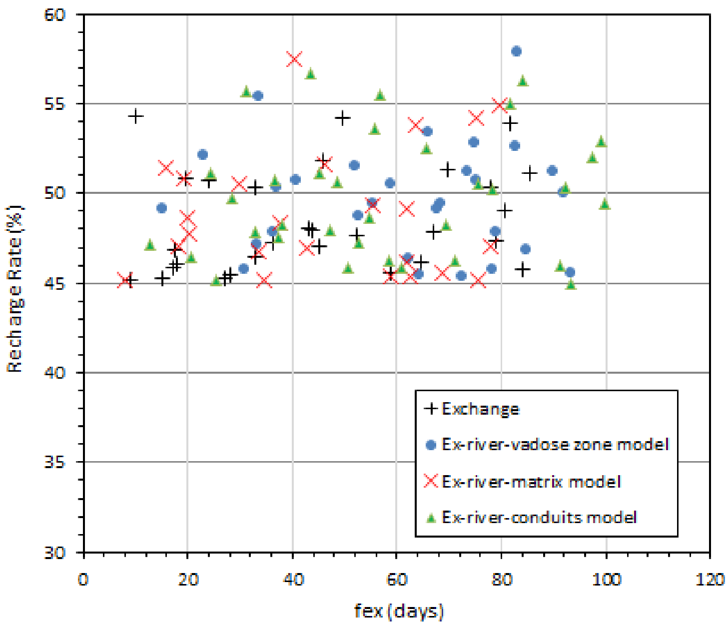

Fig 39 Recharge rate vs. Kex for all models.

Parameter f

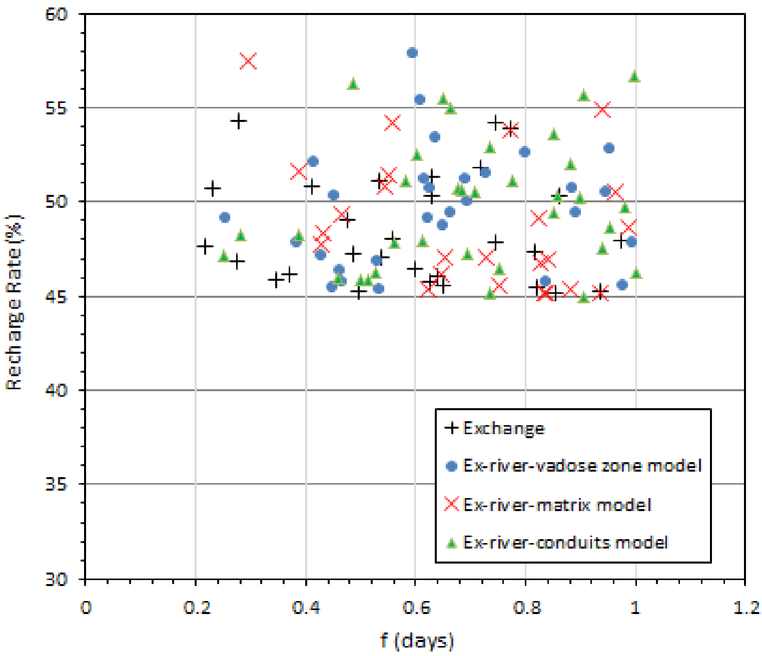

Fig 40 Recharge rate vs. f for all models.

Parameter Vmax_OS

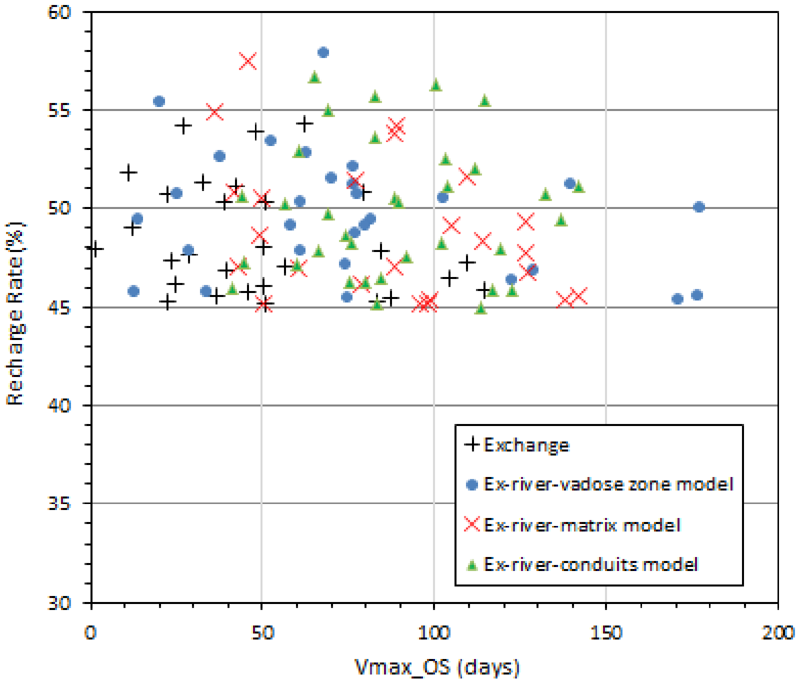

Fig 41 Recharge rate vs. Vmax_OS for all models.